Some results on the statistics of hull perimeters in large planar triangulations *and* quadrangulations

Emmanuel Guitter

▶ **To cite this version:**

Emmanuel Guitter. Some results on the statistics of hull perimeters in large planar triangulations *and* quadrangulations. Journal of Physics A: Mathematical and Theoretical, 2016, 49, pp.445203. hal-01279005

HAL Id: hal-01279005
https://hal.science/hal-01279005

Submitted on 26 Feb 2016

HAL is a multi-disciplinary open access archive for the deposit and dissemination of scientific research documents, whether they are published or not. The documents may come from teaching and research institutions in France or abroad, or from public or private research centers.

L'archive ouverte pluridisciplinaire **HAL**, est destinée au dépôt et à la diffusion de documents scientifiques de niveau recherche, publiés ou non, émanant des établissements d'enseignement et de recherche français ou étrangers, des laboratoires publics ou privés.

SOME RESULTS ON THE STATISTICS OF HULL PERIMETERS IN LARGE PLANAR TRIANGULATIONS AND QUADRANGULATIONS

EMMANUEL GUITTER

Abstract. The hull perimeter at distance d in a planar map with two marked vertices at distance k from each other is the length of the closed curve separating these two vertices and lying at distance d from the first one ($d < k$). We study the statistics of hull perimeters in large random planar triangulations and quadrangulations as a function of both k and d. Explicit expressions for the probability density of the hull perimeter at distance d, as well as for the joint probability density of hull perimeters at distances d_1 and d_2, are obtained in the limit of infinitely large k. We also consider the situation where the distance d at which the hull perimeter is measured corresponds to a finite fraction of k. The various laws that we obtain are identical for triangulations and for quadrangulations, up to a global rescaling. Our approach is based on recursion relations recently introduced by the author which determine the generating functions of so-called slices, i.e. pieces of maps with appropriate distance constraints. It is indeed shown that the map decompositions underlying these recursion relations are intimately linked to the notion of hull perimeters and provide a simple way to fully control them.

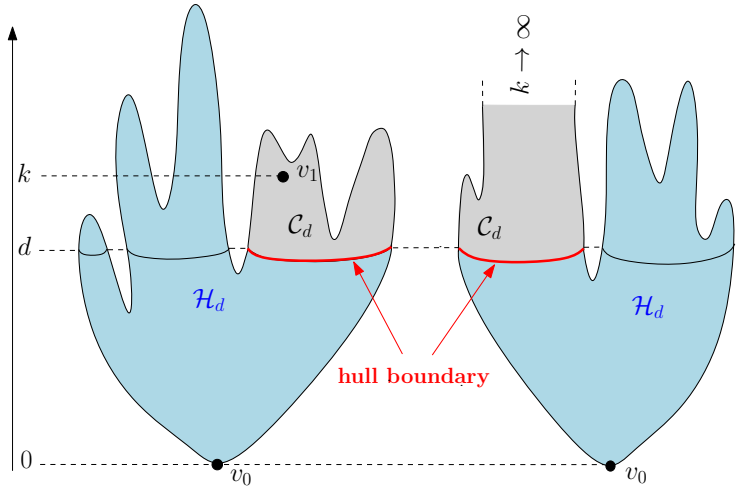

Figure 1. Left: A schematic picture of the hull boundary in a planar map with an origin v_0 and a second marked vertex v_1 at distance k from v_0. The map is represented so that vertices appear at a height equal to their distance from v_0 . The vertices at distance d from v_0 form a number of closed curves at height d, one of which separates v_0 from v_1 and constitutes the hull boundary. Right: When the map is infinite, exactly one of the connected components formed by vertices at distance larger that d is infinite. Sending $k \to \infty$ ensures that v_1 belongs to this component. This heuristic view will be made rigorous by precise definitions along the paper.

1. Introduction

Understanding the statistics of random planar maps, i.e. connected graphs embedded on the sphere, as well as their various continuous limits, such as the Brownian map [9, 8] or the Brownian plane [1], is a very active field of both combinatorics and probability theory. In this paper, we study the *statistics of hull perimeters* in large planar maps, a problem which may heuristically be understood as follows: consider a planar map $\mathcal{M}$ of some type (in the following, we shall restrict our analysis to the case of triangulations and quadrangulations) with two marked vertices, an origin vertex v_0 and a second distinguished vertex v_1 at graph distance k from v_0, for some $k \geq 2$. Consider now, for some d strictly between 0 and k, the *ball* of radius d which, so to say, is the part of the map at graph distance less than d from the origin[1]. This ball has a boundary made in general of several closed lines, each line linking vertices at distance of order d from v_0 and separating v_0 from a connected domain where all vertices are at distance larger than d (see figure 1). One of these domains $\mathcal{C}_d$ contains the second distinguished vertex v_1 and we may define the *hull* of radius d as the domain $\mathcal{H}_d = \mathcal{M} \setminus \mathcal{C}_d$, namely the union of the ball of radius d itself and of all the connected domains at distance larger than d which do not contain v_1 (see figure 1 where $\mathcal{H}_d$ is represented in light blue). The hull boundary is then the boundary of $\mathcal{H}_d$ (which is also that of $\mathcal{C}_d$), forming a closed line at distance d from v_0 and separating v_0 from v_1. The length of this boundary is called the *hull perimeter at distance* d and will be denoted by $\mathcal{L}(d)$ in the following.

The purpose of this paper is to study, as a function of both k and d, the statistics of the hull perimeter $\mathcal{L}(d)$ within uniformly drawn planar maps of some given type (here triangulations and quadrangulations) equipped with a randomly chosen pair of marked vertices at distance k from one another. Even though the combinatorics developed in this paper allows us to keep the size N (= number of faces) of the maps finite, explicit statistical laws will be presented only in the limit of *infinitely large maps*, namely when $N \to \infty$. In this case, it is expected that exactly one of the components outside the ball of radius d is infinite. In particular, sending $k \to \infty$ allows us to enforce that v_1 belongs to this infinite component so that the hull of radius d no longer depends on v_1 in this case. This limits describes a slightly simpler notion of hull boundary for vertex-pointed infinite planar maps, namely the line at distance d from the origin v_0 separating this origin from infinity (see figure 1-right).

The question of the hull perimeter statistics was already addressed in several papers [7, 6, 2, 3]. For a given choice of map ensemble, the above heuristic presentation may be transformed into a well-defined statistical problem by a rigorous definition of the hull boundary at distance d within the maps at hand. Several prescriptions may be adopted and our precise choice will be detailed in Section 2.1. This choice is different from the prescriptions used in [7, 6, 2, 3] and is thus expected to give different results for the hull perimeter statistics at finite d and k. In the limit of large d and k however, all prescriptions should eventually yield the same universal laws (up to some possible finite rescalings). This assumption is corroborated by our results on the hull perimeter probability density which precisely reproduce the expressions of [7, 6, 2, 3], as displayed in eqs. (1) and (2) below. The laws that we find for large d and k are the same for triangulations and for quadrangulations, up to a global scale change, and we expect that they should emerge for other families of maps as well.

The paper is organized as follows: we start by giving in Section 2.1 our precise definition of the hull boundary, which we view as a particular dividing line drawn on some canonical "slice" representation of the map at hand. The construction of this line is slightly different for triangulations and for quadrangulations and mimics that discussed by the author in [5, 4] in a related context. We then present our main results in Section 2.2, namely explicit expressions for the probability density of the hull perimeter in (i) the regime of a large but

[1]Several prescriptions may be used to precisely define the ball, each leading to a slightly different notion of hull.

finite d and $k \to \infty$ and (ii) the regime of large d and k with a fixed ratio $d/k < 1$, as well as for the joint probability density of the hull perimeters at two large but finite distances d_1 and d_2 for $k \to \infty$. Sections 3 and 4 are devoted to the derivation of our main results. We first recall in Section 3 the existence of a recursion relation for the generating function of the slices representing our maps and show how the map decomposition underlying this recursion may be related to our notion of hull boundary. This allows us to obtain easily a number of explicit expressions for map generating functions with a control on hull perimeters. The case of quadrangulations is discussed in Section 3.1 and that of triangulations in Section 3.2. Expansions of these generating functions are presented in Appendix B, which display the *numbers* of quadrangulations and triangulations with fixed N (= number of faces), k, d and $\mathcal{L}(d)$ for the first allowed values. We then extract in Section 4 from the singularities of the generating functions the desired hull perimeter probability densities for quadrangulations and triangulations with an infinitely large number N of faces. The details of the technique are discussed in Section 4.1 and we show in Section 4.2 how to slightly simplify the calculations for large k. Some involved intermediate formulas are given in Appendix C. The case of large d and k of the same order is discussed in Section 4.3. All over the paper, explicit expressions are first obtained for the *Laplace transforms* of the various probability densities at hand. The final step consisting in taking the desired inverse Laplace transforms is discussed in Appendix A. We gather our concluding remarks in Section 5.

2. Summary of the results

2.1. **Definition of the hull boundary in pointed-rooted triangulations and quadrangulations.** A natural way to define the hull boundary is to first construct the ball of radius d: this requires deciding which *faces* of the map are retained in the ball[2] and many inequivalent choices may be adopted, each leading to a slightly different definition of hull. In [7], Krikun gave a particularly elegant prescription in the case of triangulations, later used in [2], which allowed him to relate the hull boundary statistics to that of some "time-reversed" branching process. An alternative way to define the ball and hull of radius d, described in [3], is to use the graph distance on the dual map as a way one to assign distances directly to the faces of the original map. Here we shall use yet another prescription and *construct directly* the hull boundary at distance d without having recourse to a preliminary construction of the ball of radius d. Our approach applies to both triangulations and quadrangulations and is based on a technique developed recently in [5, 4] to compute the twopoint function of these maps.

Our starting point is an arbitrary *k-pointed-rooted* planar triangulation (respectively quadrangulation) i.e. a planar map whose all faces have degree 3 (respectively 4) endowed with a marked vertex v_0 (the origin vertex) and a marked edge e_1 (the root edge) oriented from a vertex v_1 at distance k from v_0 towards a vertex at distance $k-1$ from v_0 (see figure 2-left), for some $k \geq 1$ (respectively $k \geq 2$). The use of a pointed-rooted map rather than a simple vertex bi-pointed map (with two marked vertices v_0 and v_1) is a standard procedure which highly simplifies the underlying combinatorics. Note that, by definition, not all edges leaving a vertex v_1 at distance k from v_0 can serve as root edge for our pointed-rooted map (since we impose that e_1 necessarily points towards a vertex at distance $k-1$ from v_0) but that, for each v_1 at distance k, at least one such edge exists.

It is well-known that any k-pointed-rooted planar map, as defined above, may be bijectively transformed into a so-called *k-slice* by cutting the map along the *leftmost* shortest path[3] from v_1 to v_0 and then unwrapping the map (see figure 2-right). A k-slice is a planar

[2]As opposed to vertices which are simply characterized by their graph distance from v_0, faces may be of different types according to the graph distance of their incident vertices.

[3]This path is the sequence of edges obtained by taking e_1 as first step and then, at each encountered vertex at distance ℓ from v_0, picking the leftmost edge leading from this vertex to a vertex at distance $\ell - 1$ from v_0, until the path eventually reaches v_0.

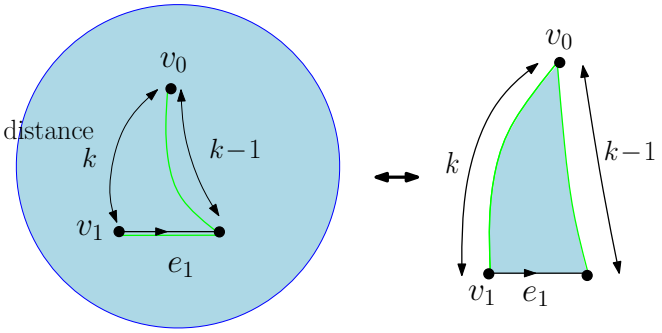

FIGURE 2. A schematic picture of a k-pointed-rooted planar map (left), i.e. a map with a marked origin v_0 and a marked edge e_1 with extremities at distance k and $k-1$ from v_0. We have drawn in green the leftmost shortest path (starting with e_1) from v_1 to v_0. Cutting along this line and unwrapping the map creates a k-slice with apex v_0 and base e_1 (right) characterized by the properties (1)-(4) of the text. The correspondence between k-pointed-rooted maps and k-slices is a bijection.

map whose all faces have a fixed degree δ (with $\delta = 3$ if the map before cutting was a triangulation or $\delta = 4$ if it was a quadrangulation), except the root face (which is the face on the right of e_1 after cutting and unwrapping) which has degree $2k$. A k-slice is characterized by the following properties:

(1) the left boundary of a k-slice, which is formed by the k edges incident to its root face lying between v_1 and v_0 clockwise around the rest of the map is a shortest path between v_1 and v_0 within the k-slice;
(2) the right boundary of a k-slice, which is formed by the $k-1$ edges incident to its root face lying between the endpoint of e_1 and v_0 counterclockwise around the rest of the map is a shortest path between these two vertices within the k-slice;
(3) the right boundary is the *unique* shortest path between its endpoints within the k-slice;
(4) the left and right boundaries do not meet before reaching v_0.

The vertex v_0 is called the *apex* and the edge e_1 the *base* of the k-slice. Clearly, due to the particular choice of cutting line, the cutting procedure applied to a k-pointed-rooted map creates a k-slice. Given this k-slice, the original k-pointed-rooted map is reconstructed by gluing the left boundary of the k-slice to the union of its base e_1 and its right boundary in the unique way which preserves the distances to v_0. The transformation between k-pointed-rooted maps and k-slices is a bijection. More simply, the k-slice with apex v_0 and base e_1 may be viewed as a canonical representation of the associated k-pointed-rooted map with origin v_0 and root edge e_1.

2.1.1. *Definition of the hull boundary in a pointed-rooted quadrangulation.* Let us now define the hull boundary of our k-pointed-rooted map. We start with the case of quadrangulations and perform our construction on the associated k-slice. Our construction is in all point similar to that discussed in [4]. Given $k \geq 3$ and d in the range $2 \leq d \leq k-1$, we start from the (unique) vertex $v_d^{(0)}$ of the right boundary of the k-slice at distance $d-1$ from v_0 and consider the face on the left of the edge connecting $v_d^{(0)}$ to its neighbor at distance $d-2$ from v_0 along the right boundary. The last two vertices incident to the face are necessarily distinct from the first two and are at distance d and $d-1$ respectively from v_0 (see figure 3). This is a direct consequence of the property (3) of the right boundary (see [4] for a detailed argument). The vertex $v_d^{(0)}$ is therefore incident to at least one edge leading to a

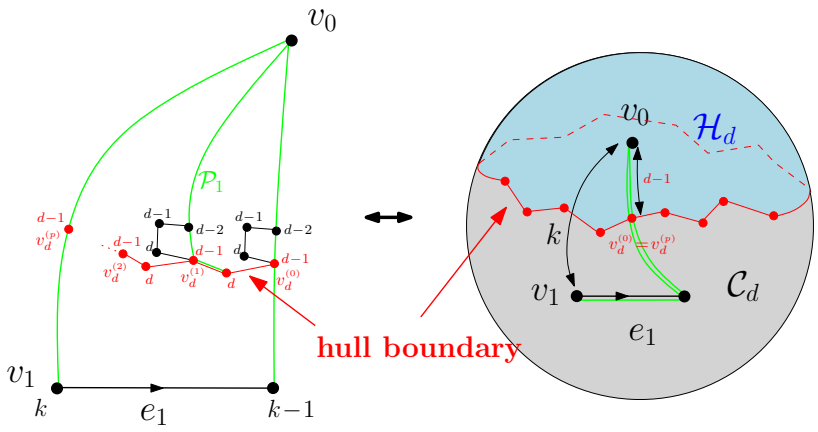

FIGURE 3. The construction of the hull boundary for quadrangulations (see text for details). The hull boundary is first constructed as an open line on the associated k-slice, then transformed into a simple closed curve on the quadrangulation by re-gluing.

neighboring vertex at distance d from v_0 itself incident to one edge leading to a vertex at distance $d-1$ from v_0 and distinct from $v_d^{(0)}$. These two edges define a *2-step path* of "type" $d-1 \to d \to d-1$ with distinct endpoints. Pick the *leftmost* such 2-step path from $v_d^{(0)}$ and call $(e_d^{(0)}, f_d^{(0)})$ the corresponding pair of successive edges, leading to a vertex $v_d^{(1)}$ at distance $d-1$ from v_0 and different from $v_d^{(0)}$. We can then draw the leftmost shortest path $\mathcal{P}_1$ from $v_d^{(1)}$ to v_0 and consider the face on the left of the edge connecting $v_d^{(1)}$ to its neighbor on $\mathcal{P}_1$ at distance $d-2$ from v_0. Repeating the argument allows us to construct a leftmost 2-step path $(e_d^{(1)}, f_d^{(1)})$ from $v_d^{(1)}$ to yet another distinct vertex $v_d^{(2)}$ and so on. As explained in [4], the line formed by the successive 2-step paths $(e_d^{(i)}, f_d^{(i)})$, $i = 0, 1, \cdots$ cannot form loops in the k-slice and necessarily ends after p iterations at the (unique) vertex $v_d^{(p)}$ at distance $d-1$ from v_0 lying on the left boundary of the k-slice[4] (see [4] for a detailed argument). This line forms our hull boundary at distance d from v_0. Indeed, upon re-gluing the k-slice into a k-pointed-rooted quadrangulation, we identify $v_d^{(0)}$ and $v_d^{(p)}$ and the line forms a simple closed curve visiting alternatively vertices at distance $d-1$ and d from v_0 and separating v_0 from v_1 (see figure 3). Clearly, all the vertices in the domain lying on the same side of the line as v_1 are at a distance larger than or equal to $d-1$ (and which can be equal to $d-1$ on the line only) and this domain constitutes what we called $\mathcal{C}_d$ in the introduction. As for the domain lying on the same side of the line as v_0, it contains all the vertices at distance less than or equal to $d-1$ from v_0 (together with other vertices at arbitrary distance) and constitutes the hull $\mathcal{H}_d$.

The hull perimeter $\mathcal{L}(d)$ is the length $2p$ of the line above. For convenience, we decide to extend our definition of the hull boundary to the case $d = 1$ and $k \geq 2$ by taking the convention that it is then reduced to the simple vertex v_0 and has length 0 accordingly, i.e.:

$$\mathcal{L}(1) = 0 \quad \text{for quadrangulations .}$$

2.1.2. *Definition of the hull boundary in a pointed-rooted triangulation.* The case of triangulations is slightly simpler and the construction follows that of [5]. We start from the k-slice associated with a given k-pointed-rooted triangulation, with now $k \geq 2$. Given d in the

[4]Note that the vertex preceding $v_d^{(p)}$ on the line, at distance d from v_0 may lie either strictly inside the k-slice or on its left boundary.

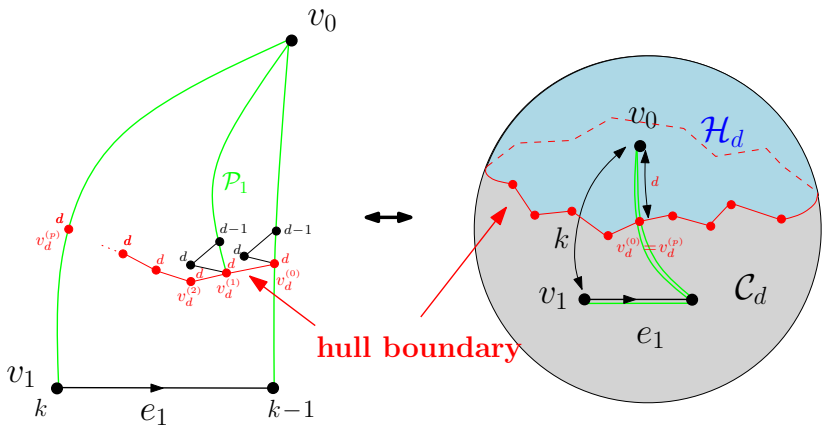

FIGURE 4. The construction of the hull boundary for triangulations (see text for details). The hull boundary is first constructed as an open line on the associated k-slice, then transformed into a simple closed curve on the triangulation by re-gluing.

range $1 \leq d \leq k-1$, we look at the (unique) vertex $v_d^{(0)}$ of the right boundary of the k-slice at distance d from v_0 and consider the triangle on the left of the edge connecting $v_d^{(0)}$ to its neighbor at distance $d-1$ from v_0 along the right boundary. The third vertex incident to the triangle is necessarily distinct from the first two and at distance d from v_0 (see figure 4). This is again a direct consequence of the property (3) of the right boundary (see [5] for a detailed argument). The vertex $v_d^{(0)}$ is therefore incident to at least one edge leading to a distinct neighbor at distance d from v_0. Call $e_d^{(0)}$ the leftmost such edge and $v_d^{(1)}$ its extremity different from $v_d^{(0)}$. We can then draw the leftmost shortest path $\mathcal{P}_1$ from $v_d^{(1)}$ to v_0 and consider the triangle on the left of the edge connecting $v_d^{(1)}$ to its neighbor on $\mathcal{P}_1$ at distance $d-1$ from v_0. Repeating the argument allows us to construct a leftmost edge $e_d^{(1)}$ to yet another distinct vertex $v_d^{(2)}$ and so on. As explained in [5], the line formed by the successive edges $e_d^{(i)}$, $i = 0, 1, \cdots$ cannot form loops in the k-slice and necessarily ends after p iterations at the (unique) vertex $v_d^{(p)}$ at distance d from v_0 lying on the left boundary of the k-slice (see [5] for a detailed argument). This line forms our hull boundary at distance d from v_0. Upon re-gluing the k-slice into a k-pointed-rooted triangulation, the line indeed forms a simple closed curve visiting only vertices at distance d from v_0 and separating v_0 from v_1. Clearly, all the vertices in the domain lying on the same side of the line as v_1 are at a distance larger than or equal to d (and which can be equal to d on the line only): this domain constitutes what we called $\mathcal{C}_d$ in the introduction. The complementary domain $\mathcal{H}_d$, lying on the same side of the line as v_0, constitutes the hull and contains all the vertices at distance less than or equal to d from v_0 together with other vertices at arbitrary distance.

The hull perimeter $\mathcal{L}(d)$ is the length p of the line above. Again, for convenience, we decide to extend our definition of the hull boundary to the case $d = 0$ and $k \geq 1$ by taking the convention that it is then reduced to the simple vertex v_0 and has length 0, namely:

$$\mathcal{L}(0) = 0 \quad \text{for triangulations .}$$

2.2. **Main results on the statistics of hull perimeters.** Having defined the hull perimeter $\mathcal{L}(d)$, our results concern the statistics of this perimeter in the ensemble of uniformly drawn k-pointed-rooted quadrangulations (respectively triangulations) having a *fixed number*

of faces N, and for a *fixed value of the parameter* k (recall that our definition of k-pointed-rooted maps imposes not only that the first extremity v_1 of their root edge e_1 is at distance k from the origin v_0 but also that the second extremity of e_1 is at distance $k-1$ from v_0). More precisely, we shall give explicit expressions *in the limit* $N \to \infty$ *of this ensemble*. Note that, when sending $N \to \infty$, k is kept finite (at least at a first stage) and *does not scale with* N. This limit is called the *local limit* of infinitely large quadrangulations (respectively triangulations). We shall denote by $P_k(\{\cdot\})$ the probability of some event $\{\cdot\}$ and $E_k(\{\cdot\})$ the expectation value of some quantity $\{\cdot\}$ in this limit. When d and k themselves become large (recall that $d \leq k-1$), we find that the perimeter $\mathcal{L}(d)$ typically scales like d^2, so we are naturally led to define the rescaled quantity:

$$L(d) \equiv \frac{\mathcal{L}(d)}{d^2} \ .$$

Let us now present the main three results of this paper on the statistics of $L(d)$.

2.2.1. *Probability density for* $L(d)$ *when* $k \to \infty$. Our first result concerns the $k \to \infty$ limit, with probabilities and expectation values denoted by $P_\infty(\{\cdot\})$ and $E_\infty(\{\cdot\})$. We insist here on the fact that, although both N and k are sent to infinity, k does not scale with N: in other words, we first send $N \to \infty$, and only then send $k \to \infty$. As mentioned in the introduction, the hull perimeter $\mathcal{L}(d)$ may then be viewed as the length of the line "at distance d" from v_0 separating v_0 from infinity. We find:

$$\lim_{d\to\infty} E_\infty(e^{-\tau L(d)}) = \frac{1}{(1+c\,\tau)^{3/2}} \ , \tag{1}$$

or equivalently (via a simple inverse Laplace transform):

$$\lim_{d\to\infty} P_\infty(L \leq L(d) < L + dL) = \frac{2}{\sqrt{\pi}} \frac{\sqrt{L}}{c^{3/2}} e^{-\frac{L}{c}}\, dL \tag{2}$$

with c taking a different value for quadrangulations and triangulations, namely:

$$\begin{cases} c = \dfrac{1}{3} & \text{for quadrangulations ,} \\ \\ c = \dfrac{1}{2} & \text{for triangulations .} \end{cases} \tag{3}$$

We recover here the precise form of the hull perimeter probability density found by Krikun [7, 6] and by Curien and Le Gall [2, 3]. The value of $c = 1/3$ that we find for quadrangulations matches that of [3][5] but is only $2/3$ of that found in [6]. This suggest that our prescription and that of [3] yield hull boundaries whose lengths are essentially the same, while the prescription used in [6] creates hull boundaries which are larger by a factor $3/2$. Our value $c = 1/2$ for triangulations is half that found in [7, 3], suggesting that our prescription yields hull boundaries whose lengths are half those of the previous studies.

Note that, we find in particular,

$$\lim_{d\to\infty} E_\infty(L(d)) = \frac{3c}{2} \ .$$

[5]The correspondence with [3] is $c = p/(4h^2)$ where $p = 2^{2/3}/3$ and $h = 1/2^{2/3}$ for quadrangulations, leading to $c = 1/3$ and $p = 1/3^{1/3}$ and $h = 1/(2 \cdot 3^{1/6})$ for triangulations, leading to $c = 1$. Although p and h are different, the same value $c = 1$ is also obtained in [3] for so-called triangulations of type II, which have no loops. These are the triangulations considered in [7] by Krikun, who also finds $c = 1$, while he gets $c = 1/2$ for quadrangulations [6].

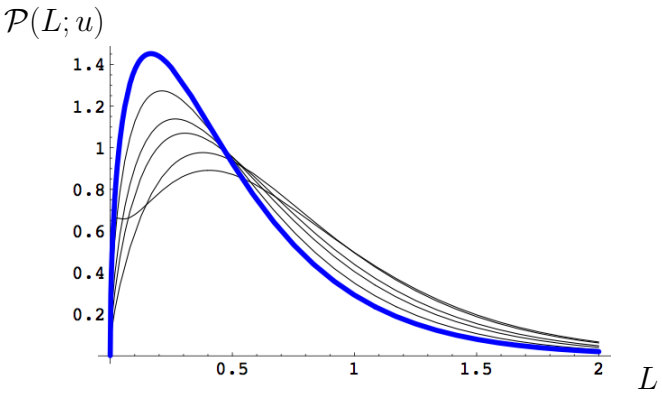

FIGURE 5. The probability density $\mathcal{P}(L;u)$ for $c=1/3$ and for $u=0$ (blue thick line) and increasing values $u=1/8$, $1/4$, $1/3$, $1/2$ and $2/3$. For this latter value, a peak starts to emerge around $L=0$.

2.2.2. *Probability density for $L(d)$ when d is a finite fraction of k.* Our second result concerns the statistics of the hull perimeter at a distance d corresponding to a *finite fraction* of the total distance k between v_0 and v_1, in the limit of large k. In other words, we consider the situation where

$$d = k\,u\ , \qquad 0<u<1\ ,$$

for some fixed u and for large k. We find that:

$$\begin{aligned}
&\lim_{k\to\infty} E_k(e^{-\tau L(k\,u)}) = F\left(\sigma(\tau;u);u\right) \quad \text{with } \sigma(\tau;u)\equiv \frac{1-2u+c\,\tau(1-u)^2}{u^2}\ ,\\
&F(\sigma;u)\equiv \left(\frac{8\sigma^4+47\sigma^3+90\sigma^2+120\sigma+48}{4(\sigma+1)^{5/2}}-12\right)\frac{u^3}{\sigma^3}\\
&\qquad +\left(\frac{4\sigma^4+19\sigma^3+30\sigma^2+68\sigma+32}{4(\sigma+1)^{5/2}}+3\sigma-8\right)\frac{u(1-2u)}{\sigma^3}\\
&\qquad +\left(\frac{4\sigma^5+16\sigma^4-7\sigma^2-40\sigma-24}{4(\sigma+1)^{5/2}}+3\sigma^2-5\sigma+6\right)\frac{(1-2u)(1-u)^2\left(1-2u+2u^2\right)}{\sigma^4u^3}\ ,
\end{aligned} \tag{4}$$

with c as in (3) above.

Note that, for $\tau\geq 0$ and $0<u<1$, $\sigma(\tau;u)+1=(1+c\,\tau)(1-u)^2/u^2>0$ so that the denominator $(\sigma+1)^{5/2}$ in (4) does not vanish. For $0<u<1/2$, we have the stronger property $\sigma(\tau;u)>0$ and $F\left(\sigma(\tau;u);u\right)$ therefore clearly has no singularity for $\tau\geq 0$. For $1/2<u<1$ however, $\sigma(\tau;u)$ vanishes at the non-negative value $\tau=\frac{2u-1}{c\,(1-u)^2}$ and $F\left(\sigma(\tau;u);u\right)$ may seem at a first glance to develop some singularity there. Such behavior is not allowed for the Laplace transform of some probability density so a closer look at the formula is required. Expanding $F(\sigma;u)$ around $\sigma=0$ shows that $F(\sigma;u)$ is in fact well-behaved around $\sigma=0$ with $F(\sigma;u)=(512u^6-3012u^5+7518u^4-10020u^3+7515u^2-3006u+501)/(64u^3)+O(\sigma)$. The seeming singularity at $\tau=\frac{2u-1}{c\,(1-u)^2}$ is therefore only an illusion.

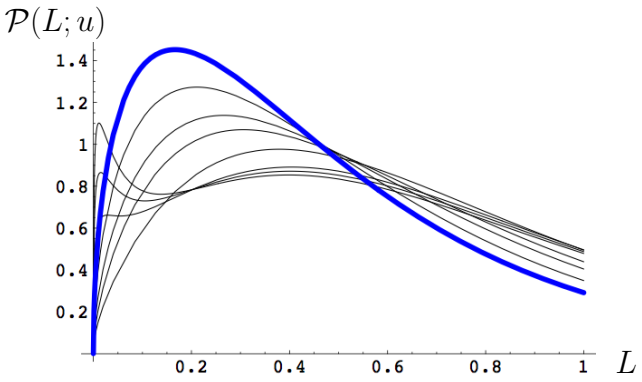

FIGURE 6. The same plot as figure 5 limited to the range $0 \leq L \leq 1$, with two new value $u \simeq 0.69$ and $u \simeq 0.71$. This plot is to emphasize the emergence of a peak for small L when $u \geq 1/2$.

Via an inverse Laplace transform, whose details are discussed in Appendix A, eq. (4) is equivalent to[6]

$$\lim_{k\to\infty} P_k(L \leq L(k\,u) < L + dL) = \mathcal{P}(L;u)\,dL$$

$$\text{with } \mathcal{P}(L;u) = \frac{2}{\sqrt{\pi}}\frac{\sqrt{L}}{c^{3/2}}e^{-\frac{L}{c}} \times \frac{\left(e^{\frac{L}{c\,b}}\sqrt{\frac{\pi L}{c\,b}}\left(1-\mathrm{erf}\left(\sqrt{\frac{L}{c\,b}}\right)\right)-1\right)p\left(\frac{L}{c\,b}\right)+r\left(\frac{L}{c\,b}\right)}{4\,(\sqrt{b}+b)^3} \tag{5}$$

$$\text{where } b \equiv\ b(u) = \frac{(1-u)^2}{u^2}\ ,$$

$$p(\ell) \equiv 2b\left(b^2-1\right)\ell^2 - \left(5b^3+3b+4\right)\ell + 6\left(b^3-1\right)\ ,$$

$$r(\ell) \equiv b\left(15b^2-1\right)\ell + 2\left(5b^3-1\right)\ .$$

The function $\mathcal{P}(L;u)$ is plotted in figure 5 for various values of u and $c = 1/3$. The limit $u \to 0$ (i.e $b \to \infty$) describes situations where the distance d at which the hull perimeter is measured does not scale with k, so we expect to recover the result of eq. (2) in this limit. This is indeed the case as:

$$\mathcal{P}(L;0) = \frac{2}{\sqrt{\pi}}\frac{\sqrt{L}}{c^{3/2}}e^{-\frac{L}{c}}\ .$$

The probability density $\mathcal{P}(L;0)$ is displayed in blue in figure 5 (thick line). Note that $\mathcal{P}(L;u)/\mathcal{P}(L;0)$ is a function of the variable

$$R \equiv \frac{L}{b(u)} = L\,\frac{u^2}{(1-u)^2} = L\,\frac{d^2}{(k-d)^2}\ .$$

Recall that $L(d)$ is the ratio of the the actual hull perimeter $\mathcal{L}(d)$ by its "natural scale" d^2. The new variable R therefore corresponds to probing the value of the random variable

$$R(d) \equiv \frac{\mathcal{L}(d)}{(k-d)^2}\ ,$$

i.e. measuring the hull perimeter at a scale no longer fixed by d^2 by rather by $(k-d)^2$. When u becomes larger than $1/2$, a peak for small L starts to emerge in $\mathcal{P}(L,u)$, as displayed in

[6]Here $\mathrm{erf}(a)$ denotes the usual error function $(2/\sqrt{\pi})\int_0^a e^{-z^2}\,dz$.

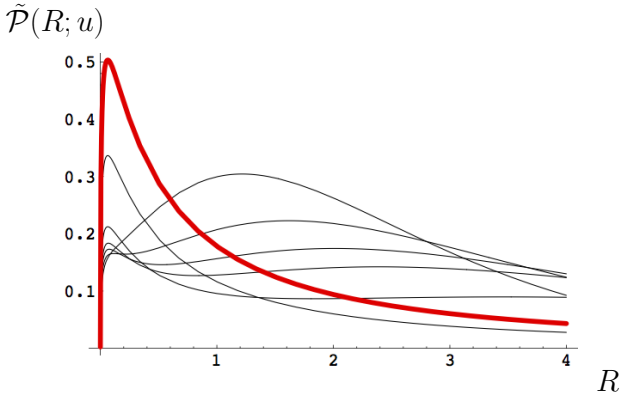

FIGURE 7. The probability density $\tilde{\mathcal{P}}(R;u)$ for $c=1/3$ and for $u\simeq 0.64$, 0.67, 0.69, 0.71, 0.75, 0.875 and $u=1$ (red thick line). The height of the peak for small L increases with increasing u.

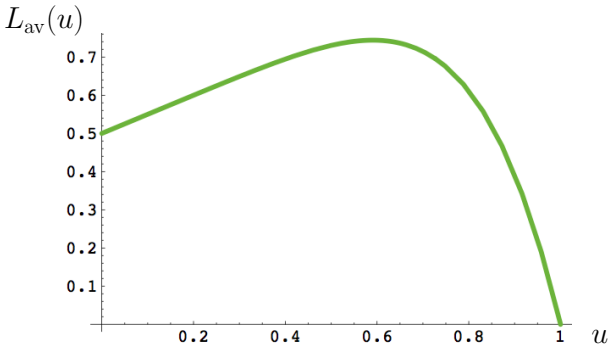

FIGURE 8. The average value $L_{\rm av}(u)\equiv\lim_{k\to\infty}E_k(L(k\,u))$ as a function of u (here $c=1/3$).

figure 6. This peak increases when u tends to 1 ($b\to 0$). This limit is best captured by switching to the variable R, namely considering

$$\lim_{k\to\infty} P_k(R\le R(k\,u)<R+dR)=\tilde{\mathcal{P}}(R;u)\,dR \quad \text{with} \quad \tilde{\mathcal{P}}(R;u)=b\,\mathcal{P}(b\,R;u)\ .$$

In other words, when d approaches k, the natural scale for $\mathcal{L}(d)$ is no longer d^2 but rather $(k-d)^2$. The probability density $\tilde{\mathcal{P}}(R,u)$ is displayed in figure 7 for $c=1/3$ and various values of u. When $u\to 1$ ($b\to 0$), $\tilde{\mathcal{P}}(R;u)$ converges to a well-defined distribution

$$\tilde{\mathcal{P}}(R;1)=2\sqrt{\frac{R}{\pi c^5}}(R+c)-\frac{R}{c^3}\,(2R+3c)\,e^{\frac{R}{c}}\left(1-\mathrm{erf}\left(\sqrt{\frac{R}{c}}\right)\right)\ .$$

This distribution is displayed in red in figure 7 (thick line). Note that this distribution has all its moments *infinite*.

This result may appear strange at a first glance but the divergence of, say the first moment is in fact consistent with a direct computation of the average values of $L(d)$ and $R(d)$ for arbitrary u: expanding eq. (4) at first order in τ, we have indeed

$$L_{\rm av}(u)\equiv\lim_{k\to\infty}E_k(L(k\,u))=\frac{3c}{2}(1+u-3u^6+u^7)$$

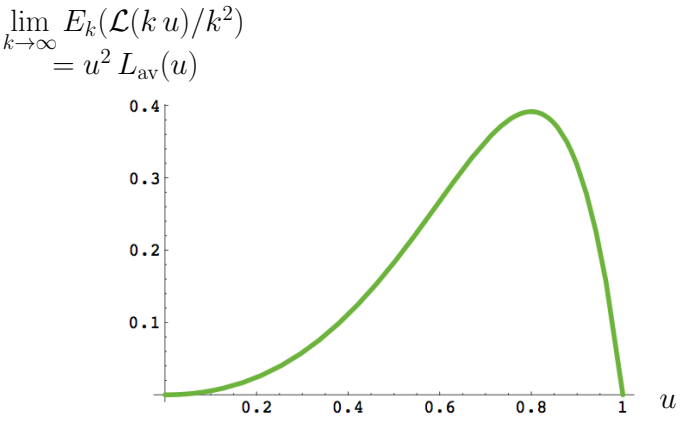

FIGURE 9. The average profile of the hull perimeter, i.e. the quantity $\lim_{k\to\infty} E_k(\mathcal{L}(k\,u)/k^2) = u^2\,L_{\rm av}(u)$ as a function of u (here $c = 1/3$).

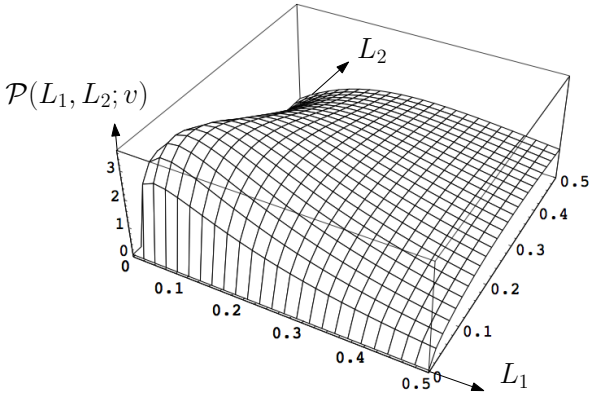

FIGURE 10. The joint probability density $\mathcal{P}(L_1, L_2; v)$ for $v = 2$ (here $c = 1/3$).

The average value $L_{\rm av}(u)$ is displayed in figure 8 for $u < 0 < 1$ and $c = 1/3$. When $u \to 0$, it tends to a finite value $3c/2$, meaning that the average hull perimeter at distance d from the origin scales like $3c/2 \times d^2$ when k is infinitely large, as expected. When d corresponds to a finite fraction $u < 1$ of k, the average hull perimeter remains of order d^2 with a finite prefactor $L_{\rm av}(u)$ depending on u. When $d \to k$ however, i.e. $u \to 1$, then $L_{\rm av}(u) \sim 15c(1-u)$ hence the average hull perimeter vanishes like $15c\,k(k-d)$. This vanishing is not surprising since the hull perimeter is also the length of the boundary of the domain $\mathcal{C}_d$ in which the vertex v_1 is "trapped". When d approaches k, this domain becomes smaller and smaller and so does its boundary. This vanishing is only linear in $(k-d)$ and the average value of $R(d)$ behaves accordingly as $15c\,k^3/(k-d)$, hence diverges when $d \to k$.

We may finally consider the average "profile" of the hull perimeter, i.e. the average value $E_k(\mathcal{L}(k\,u)/k^2)$ of the hull perimeter at distance $d = k\,u$ normalized for all u by the same *global scale* k^2 (instead of the local natural scale $(k\,u)^2$). In the limit $k \to \infty$, it is simply equal to $u^2\,L_{\rm av}(u)$ and has the form displayed in figure (9).

2.2.3. *Joint probability density for $L(d_1)$ and $L(d_2)$ when $k \to \infty$.* Our third main result deals with the joint law for hull perimeters at distances d_1 and d_2 from v_0, with again

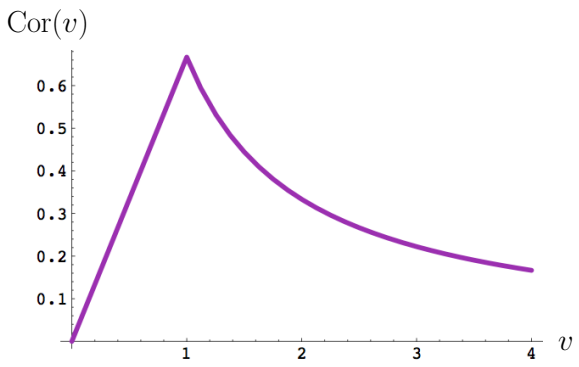

FIGURE 11. The correlation $\mathrm{Cor}(v)$ as a function of v. This quantity is independent of c.

$k \to \infty$. Assuming $d_2 > d_1$, we set:

$$d_1 = d\ , \quad d_2 = v\,d\ , \qquad \text{with } v > 1\ .$$

We find that:

$$\lim_{d\to\infty} E_\infty(e^{-\tau_1 L(d)-\tau_2 L(vd)})$$

$$= \frac{v^3}{\left(v^2(1+c\,\tau_1)(1+c\,\tau_2)-2\,v\,c\,\tau_2\left(1+c\,\tau_1-\sqrt{1+c\,\tau_1}\right)+c\,\tau_2\left(2+c\,\tau_1-2\sqrt{1+c\,\tau_1}\right)\right)^{3/2}} \tag{6}$$

which equivalently yields a joint probability density (see Appendix A for details on the appropriate double inverse Laplace transform):

$$\lim_{d\to\infty} P_\infty\Big(L_1 \le L(d) < L_1 + dL_1 \text{ and } L_2 \le L(v\,d) < L_2 + dL_2\Big) = \mathcal{P}(L_1, L_2; v)\, dL_1\, dL_2\ ,$$

$$\mathcal{P}(L_1, L_2; v) = \frac{2}{\sqrt{\pi}}\frac{\sqrt{L_1}}{c^{3/2}} e^{-\frac{L_1}{c}} \times \frac{\sqrt{2}}{c}\frac{v^2 e^{-\frac{L_2\,v^2}{c\,(v-1)^2}}}{(v-1)^2} \sum_{n=0}^{\infty} \frac{(-1)^n \left(\frac{L_1}{c(v-1)^2}\right)^{\frac{n}{2}} \pi_n\left(\sqrt{\frac{2L_2\,v^2}{c\,(v-1)^2}}\right)}{(n+1)!\,\Gamma\left(\frac{n+1}{2}\right)}\ . \tag{7}$$

Here $\pi_n(t)$ is the polynomial (of the Hermite type) defined by[7]

$$\pi_n(t) \equiv -e^{\frac{t^2}{2}} \frac{d^{n+1}}{dt^{n+1}}\left(t^n\, e^{-\frac{t^2}{2}}\right)\ . \tag{8}$$

The joint probability density $\mathcal{P}(L_1, L_2; v)$ is plotted for $v = 2$ in figure 10.

Expanding eq. (6) at first order in τ_1 and τ_2, we immediately get

$$\lim_{d\to\infty} E_\infty(L(d)\,L(v\,d)) = \frac{3}{4}c^2\left(3+\frac{2}{v}\right) \text{ for } v > 1$$

hence, by dividing by the common average value $3c/2$ for $L(d)$ and $L(v\,d)$ (and using an obvious symmetry to extend the result to $v < 1$), a correlation

$$\mathrm{Cor}(v) \equiv \frac{\lim_{d\to\infty} E_\infty(L(d)\,L(v\,d))}{\lim_{d\to\infty} E_\infty(L(d)) \times \lim_{d\to\infty} E_\infty(L(v\,d))} - 1 = \frac{2}{3\max(v, 1/v)} \qquad \text{for all } v > 0\ .$$

Note that this correlation is independent of c. The value $2/3$ at $v = 1$ is obtained directly from eq. (1). The correlation $\mathrm{Cor}(v)$ is plotted in figure 11 for illustration.

[7] The first polynomials are $\pi_0(t) = t$, $\pi_1(t) = t(3 - t^2)$, $\pi_2(t) = t(12 - 9t^2 + t^4)$, $\pi_3(t) = t(60 - 75t^2 + 18t^4 - t^6)$.

Another measure of the correlation is the average value $L_{\rm av}(v|L_1)$ of $L(d\,v)$, knowing that $L(d)$ lies in the range $[L_1, L_1+dL_1]$. By integrating $L_2\,\mathcal{P}(L_1,L_2;v)$ over L_2, it is easily found to be[8]:

$$L_{\rm av}(v|L_1) = \frac{3c\,(v-1)^2 + 3\sqrt{\pi\,c\,L_1}\,(v-1) + 2\,L_1}{2v^2}\ , \qquad v>1\ ,$$

which varies from $L_{\rm av}(1|L_1)=L_1$ to $L_{\rm av}(\infty|L_1)=3c/2$, as expected.

3. The slice recursion and the hull perimeter

We now come to the derivation of our various results. It relies on the existence of a recursion relation for slice generating functions, as described in [4] for quadrangulatiions and [5] for triangulations. As we shall see, the origin of this recursion is indeed intimately linked to the notion of hull boundary and this will eventually allows us to have a direct control on the hull perimeter.

3.1. **The case of quadrangulations.**

3.1.1. *The slice recursion.* We consider here the k-slices defined in Section 2.1 in correspondence with k-pointed-rooted quadrangulations, and more generally the larger set of ℓ-slices with $1\le\ell\le k$. Recall that, in an ℓ-slice, ℓ is the length of its left boundary and is also the distance $d(v_0,v_1)$ between its apex and the first extremity of its base. Let us denote by $R_k^{(q)}\equiv R_k^{(q)}(g)$, $k\ge 1$, the generating function for this larger family of slices, where we assign a weight g to each tetravalent *inner* face (i.e. each face other than the outer face). The quantity $R_k^{(q)}$ is also the generating function, with a weight g per face, of pointed-rooted quadrangulations[9] whose graph distance $d(v_0,v_1)$ between the origin v_0 and the first extremity v_1 of the root edge satisfies $1\le d(v_0,v_1)\le k$. The explicit expression for $R_k^{(q)}$ can be found in [4] and reads:

$$R_k^{(q)} = R^{(q)}\,\frac{(1-x^k)(1-x^{k+3})}{(1-x^{k+1})(1-x^{k+2})}\ , \qquad R^{(q)}=\frac{1-\sqrt{1-12g}}{6g}\ ,$$

where x is a parametrization of g through

$$g=\frac{x(1+x+x^2)}{(1+4x+x^2)^2}\ .$$

Note that x and $1/x$ lead to the same value of g so we shall impose the extra condition $|x|\le 1$ to univocally fix x. The generating functions are well-defined for real g in the range $0\le g\le 1/12$: this then corresponds to a real x in the range $0\le x\le 1$. To be precise, the recursion relation found in [4] concerns the quantity

$$T_k^{(q)}\equiv R_k^{(q)} - R_1^{(q)}\ , \qquad k\ge 1\ ,$$

which enumerates ℓ-slices whose left boundary length ℓ is between 2 and k (note that $T_1^{(q)}=0$). From the explicit expression of $R_k^{(q)}$, we immediately deduce

$$T_k^{(q)} = T^{(q)}\,\frac{(1-x^{k-1})(1-x^{k+4})}{(1-x^{k+1})(1-x^{k+2})}\ , \qquad T^{(q)}=\frac{x(1+4x+x^2)}{(1+x+x^2)^2}\ .$$

[8] It is easily verified that, when computing the p-th moment of L_2 with the distribution $\mathcal{P}(L_1,L_2;v)$, only the first $2p+1$ polynomials π_n (i.e. $n=0,\cdots,2p$) in (7) give a non-zero contribution.

[9] By pointed-rooted quadrangulations, we mean in general ℓ-pointed-rooted quadrangulations with arbitrary $\ell\ge 1$.

It was shown in [4] that this generating function satisfies a recursion relation of the form:

$$\begin{aligned} &T_k^{(q)} = \mathcal{K}^{(q)}(T_{k-1}^{(q)}) \ , \\ &\mathcal{K}^{(q)}(T) = \frac{(R_1^{(q)})^2(T+R_1^{(q)})\,\Phi^{(q)}(T)}{1-R_1^{(q)}(T+R_1^{(q)})\,\Phi^{(q)}(T)} \ , \ \Phi^{(q)}(T) \equiv \Phi^{(q)}(T,g) = \sum_{i\geq 2} h_{2i}^{(q)}(g)\,T^{i-2} \ , \end{aligned} \tag{9}$$

for $k \geq 2$ with $T_1^{(q)} = 0$. Here $h_{2i}^{(q)}(g)$ are appropriate generating functions whose definition can be found in [4] and whose explicit expression will not be needed in our calculation. The precise form of the "kernel" $\mathcal{K}^{(q)}(T)$ is also not important for our calculation and we displayed it only to help the reader make the connection with [4]. What matters for us is only the following simple property: the kernel $\mathcal{K}^{(q)}(T)$ is independent of k whereas $T_k^{(q)}$ depends on k only through the variable x^k. We immediately deduce that, if we make the transformation $x^k \to \lambda x^k$ in the expressions for $T_k^{(q)}$, the obtained quantity still satisfies the same recursion relation. In other words, if we set

$$T_k^{(q)}(\lambda) = T^{(q)}\frac{(1-\lambda\,x^{k-1})(1-\lambda\,x^{k+4})}{(1-\lambda\,x^{k+1})(1-\lambda\,x^{k+2})} \ , \tag{10}$$

then $T_k^{(q)}(\lambda)$ still satisfies[10]

$$T_k^{(q)}(\lambda) = \mathcal{K}^{(q)}(T_{k-1}^{(q)}(\lambda)) \ . \tag{11}$$

This, together with the explicit form (10) of $T_k^{(q)}(\lambda)$ is the only ingredient that we shall rely on in the following for our explicit calculations.

3.1.2. *Connection with the hull perimeter.* Let us now briefly recall the origin of the recursion relation and show how it may allow us to control the hull perimeter. Starting with an ℓ-slice with left boundary length ℓ between 2 and k (as enumerated by $T_k^{(q)}$), the recursion is obtained by cutting the ℓ-slice along some particular line, called the "dividing line" in [4]. This dividing line is precisely the hull boundary *at distance* $\ell - 1 = d(v_0, v_1) - 1$ from v_0 in the ℓ-slice, as we defined it in Section 2.1[11] (see figure 12). The generating function $T_k^{(q)}$ is obtained by multiplying the generating function of the domain $\mathcal{C}_{\ell-1}$ (corresponding in the slice to the domain on the same side of the hull boundary as v_1) by the generating function of the domain $\mathcal{H}_{\ell-1}$ (corresponding in the slice to the domain on the same side of the boundary as v_0). For a *fixed value* $\mathcal{L}$ of the hull perimeter $\mathcal{L}(\ell-1)$, the first generating function is easily seen to be independent of ℓ (since there is no restriction on mutual distances within this domain apart from the fact that v_1 is at distance 1 from the boundary). This generating function is nothing but (see [4] for details):

$$[T^{\mathcal{L}/2}]\mathcal{K}^{(q)}(T)$$

(recall that $\mathcal{L}$ is even). As for the domain $\mathcal{H}_{\ell-1}$, it is formed of *exactly* $\mathcal{L}/2$ *slices* with respective left boundary lengths $\ell_1, \ell_2, \cdots, \ell_{\mathcal{L}/2}$, each satisfying $2 \leq \ell_i \leq \ell - 1$, hence $2 \leq \ell_i \leq k-1$ when we sum over all possible values of ℓ between 2 and k. These slices are obtained by decomposing the domain $\mathcal{H}_{\ell-1}$ upon cutting along the leftmost shortest paths to v_0 from the $\mathcal{L}/2-1$ vertices of its boundary which are at distance $\ell-1$ from v_0, but the last one[12]. Note that when $\ell = 2$, the hull boundary at distance $\ell-1=1$ must be understood as reduced to the single vertex v_0, having length 0. Each of the $\mathcal{L}/2$ slices composing the

[10] A detailed calculation shows that this actually holds only for λ close enough to 1 so that we are guaranteed that $\frac{(1-\lambda^2\,x^{2k+1})}{(1-\lambda\,x^k)(1-\lambda\,x^{k+1})}$ remains non-negative. We shall be in this regime in the following.

[11] In [4], a first edge of the right boundary of the slice, linking its vertices $v_0^{(\ell)}$ and $v_0^{(\ell-1)}$ at respective distances $\ell-1$ and $\ell-2$ from v_0 was added for convenience to the dividing line. This edge is not present in our definition where we let the dividing line start at the vertex $v_0^{(\ell-1)}$ at distance $\ell-2$.

[12] The leftmost shortest path from this last vertex to v_0 follows the left boundary of the original ℓ-slice and need not being cut.

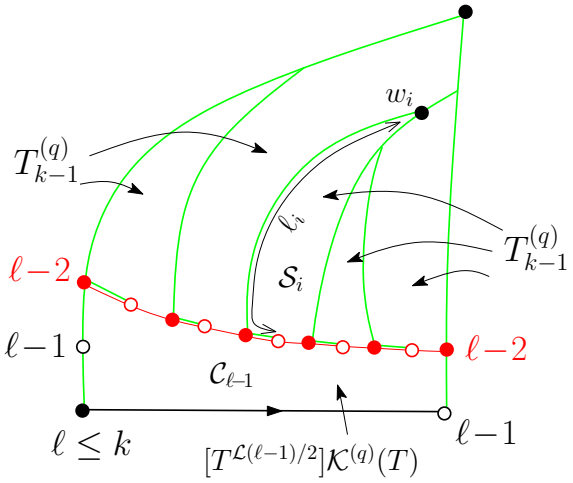

FIGURE 12. The decomposition of a slice enumerated by $T_k^{(q)}$ leading to the recursion relation (9). The hull boundary at distance $\ell-1$, represented in red and made of an alternating sequence of vertices at distance $\ell-2$ (filled red circles) and at distance $\ell-1$ (open red circles) from the apex, serves as a dividing line of even length $\mathcal{L}(\ell-1)$ (here equal to 10) separating a domain $\mathcal{C}_{\ell-1}$ from the hull. By drawing the leftmost shortest paths to the apex from each of the vertices at distance $\ell-1$ along the hull boundary (open red circles), the hull itself is decomposed into a number $\mathcal{L}(\ell-1)/2$ of sub-slices, each enumerated by $T_{k-1}^{(q)}$ (since each sub-slice $\mathcal{S}_i$ has a left boundary length ℓ_i satisfying $2 \le \ell_i \le k-1$). The generating function of the domain $\mathcal{C}_{\ell-1}$ is $[T^{\mathcal{L}(\ell-1)/2}]\mathcal{K}^{(q)}(T)$.

domain $\mathcal{H}_{\ell-1}$ is thus enumerated by $T_{k-1}^{(q)}$ and the net contribution of this domain to $T_k^{(q)}$ is eventually

$$\left(T_{k-1}^{(q)}\right)^{\mathcal{L}/2} .$$

Summing over all (even) values of $\mathcal{L}$ yields the desired recursion relation (9).

If we now wish to keep a control on the value $\mathcal{L}$ of the hull perimeter at distance $d(v_0,v_1)-1$ in the original ℓ-slices (characterized by $2 \le d(v_0,v_1) \le k$) by assigning, say a weight $\alpha^{\mathcal{L}}$ to these ℓ-slices, we simply need to replace $T_{k-1}^{(q)}$ by $\alpha^2\, T_{k-1}^{(q)}$ at the step $k-1 \to k$ of the recursion. In other words, the generating function of ℓ-slices with $2 \le \ell \le k$, with a weight g per inner face and a weight $\alpha^{\mathcal{L}(\ell-1)}$ is simply given by

$$\sum_{\substack{\mathcal{L}\ge 0 \\ \mathcal{L} \text{ even}}} [T^{\mathcal{L}/2}]\mathcal{K}^{(q)}(T) \times \alpha^{\mathcal{L}} \times \left(T_{k-1}^{(q)}\right)^{\mathcal{L}/2} = \mathcal{K}^{(q)}(\alpha^2\, T_{k-1}^{(q)}) .$$

In the argument leading to this formula, ℓ-slices with $\ell=2$ must be understood as having $\mathcal{L}(\ell-1)=0$ (since the hull boundary is reduced to v_0 in this case), in agreement with our general convention $\mathcal{L}(1)=0$ for slices associated with quadrangulations. The 2-slices are thus enumerated with a weight $\alpha^{\mathcal{L}(1)}=1$.

3.1.3. *Controlling the hull perimeter at some arbitrary d.* If we wish instead to control the hull perimeter at distance $\ell-2$ from the apex v_0 in ℓ-slices with $3 \le \ell \le k$, we may simply repeat our construction within each of the $\mathcal{L}(\ell-1)/2$ sub-slices $\mathcal{S}_i$ forming the domain $\mathcal{H}_{\ell-1}$

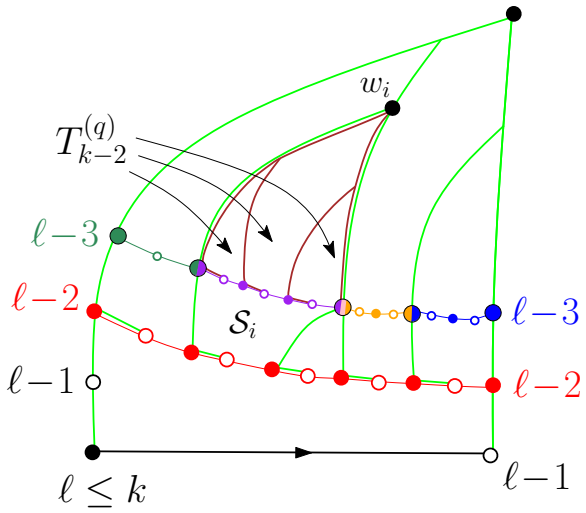

FIGURE 13. The construction of the hull boundary at distance $\ell-2$ (i.e. formed by an alternating sequence of vertices at distance $\ell-3$ and $\ell-2$) by concatenating the hull boundaries at distance ℓ_i-1 (represented in different colors) of the various sub-slices $\mathcal{S}_i$ forming $\mathcal{H}_{\ell-1}$.

(recall that the left boundary length ℓ_i of the sub-slice $\mathcal{S}_i$ satisfies $2 \leq \ell_i \leq k-1$). More precisely we start by constructing the hull boundary at distance ℓ_i-1 within each sub-slice $\mathcal{S}_i$. Here the distances within the sub-slice $\mathcal{S}_i$ are measured *from its apex* w_i which serves as origin of the sub-slice. In particular, if $\ell_i=2$ for some i, its hull boundary is reduced to the vertex w_i. The hull boundary at distance $\ell-2$ is then obtained by *concatenating* all the hull boundaries at distance ℓ_i-1 of the successive sub-slices $\mathcal{S}_i$ (see figure 13)[13]. This property is a direct consequence of the fact that the notions of distances and leftmost shortest paths within the ℓ-slice are strictly bound to the same notions within the sub-slices $\mathcal{S}_i$. In particular, even though the apex w_i of $\mathcal{S}_i$ is in general distinct from v_0, the distance $d(v_0,v)$ from v_0 to any vertex v inside $\mathcal{S}_i$ is equal to $d(v_0,w_i)$ plus the distance *within the slice* $\mathcal{S}_i$ from w_i to v: this is a direct consequence of the fact that the sub-slice boundaries are shortest paths from their base extremities to v_0 in the original ℓ-slice.

To summarize, the boundary perimeter $\mathcal{L}(\ell-2)$ is the sum of the hull perimeters at distance ℓ_i-1 of the $\mathcal{L}(\ell-1)/2$ sub-slices $\mathcal{S}_i$ forming the domain $\mathcal{H}_{\ell-1}$. As before, each of these sub-slice hull perimeters corresponds to twice the number of sub-sub-slices forming the hull at distance ℓ_i-1 of the sub-slice $\mathcal{S}_i$ at hand, each sub-sub-slice being now enumerated by $T^{(q)}_{k-2}$ (see figure 13). Considering two consecutive steps of our recursion relation, we deduce that the quantity

$$\mathcal{K}^{(q)}\left(\mathcal{K}^{(q)}\left(\alpha^2\, T^{(q)}_{k-2}\right)\right) - \mathcal{K}^{(q)}(0).$$

is the generating function of ℓ-slices with $3 \leq \ell \leq k$ with a weight g per inner face and a weight $\alpha^{\mathcal{L}(\ell-2)}$. As before, we have taken the convention that ℓ-slices with $\ell=3$ have perimeter $\mathcal{L}(\ell-2)=0$ (since their hull boundary is reduced to v_0). The subtracted term $\mathcal{K}^{(q)}(0)=T^{(q)}_1$ suppresses the ℓ-slices with $\ell=2$ which would otherwise be present from the

[13]Note that when $\ell_i=2$ for some i, the hull boundary at distance $\ell-2$ simply passes through the apex w_i without entering the sub-slice $\mathcal{S}_i$, hence contributes 0 to the hull perimeter.

first term. We may instead consider the un-subtracted quantity

$$\mathcal{K}^{(q)}\left(\mathcal{K}^{(q)}\left(\alpha^2\, T^{(q)}_{k-2}\right)\right)$$

which is the generating function of ℓ-slices with $2 \le \ell \le k$ with a weight g per inner face and a weight $\alpha^{\mathcal{L}(\ell-2)}$ *if* $\ell > 2$ (and no α-dependent weight otherwise) . Repeating the argument, we may, for $1 \le m < k$, identify

$$\underbrace{\mathcal{K}^{(q)}\big(\mathcal{K}^{(q)}\big(\cdots\big(\mathcal{K}^{(q)}\big(}_{m \text{ times}}\alpha^2\, T^{(q)}_{k-m}\big)\big)\big)\big) \tag{12}$$

as the generating function of ℓ-slices with $2 \le \ell \le k$ with a weight g per inner face and a weight $\alpha^{\mathcal{L}(\ell-m)}$ whenever $\ell > m$.

Assuming now $k \ge 3$ and d in the range $2 \le d \le k-1$, the generating function of k-slices with a weight g per inner face and a weight $\alpha^{\mathcal{L}(d)}$ is given by

$$\underbrace{\mathcal{K}^{(q)}\big(\mathcal{K}^{(q)}\big(\cdots\big(\mathcal{K}^{(q)}\big(}_{k-d \text{ times}}\alpha^2\, T^{(q)}_{d}\big)\big)\big)\big) - \underbrace{\mathcal{K}^{(q)}\big(\mathcal{K}^{(q)}\big(\cdots\big(\mathcal{K}^{(q)}\big(}_{k-d \text{ times}}\alpha^2\, T^{(q)}_{d-1}\big)\big)\big)\big)\ . \tag{13}$$

Indeed, the first term corresponds to $m = k-d$ in (12) hence enumerates ℓ-slices with $2 \le \ell \le k$ with a weight $\alpha^{\mathcal{L}(d+\ell-k)}$ if $d+\ell-k > 0$ while the second term corresponds to taking $k \to k-1$ and $m = k-d$ in (12) hence enumerates ℓ-slices with $2 \le \ell \le k-1$ with *the same weight* $\alpha^{\mathcal{L}(d+\ell-k)}$ if $d+\ell-k > 0$. Taking the difference selects precisely ℓ-slices with $\ell = k$, enumerated with a weight $\alpha^{\mathcal{L}(d)}$ (the condition $d > 0$ is automatic since we assumed $d \ge 2$).

Each of the term in the equation above may be computed as follows: define $\lambda^{(q)}(\alpha; d)$ as the solution of the equation

$$T^{(q)}_d(\lambda^{(q)}(\alpha; d)) = \alpha^2\, T^{(q)}_d$$

or equivalently

$$\frac{(1-\lambda^{(q)}(\alpha;d)\, x^{d-1})(1-\lambda^{(q)}(\alpha;d)\, x^{d+4})}{(1-\lambda^{(q)}(\alpha;d)\, x^{d+1})(1-\lambda^{(q)}(\alpha;d)\, x^{d+2})} = \alpha^2\, \frac{(1-x^{d-1})(1-x^{d+4})}{(1-x^{d+1})(1-x^{d+2})}\ . \tag{14}$$

This equation is quadratic in $\lambda^{(q)}(\alpha; d)$ and we have to pick the branch of solution satisfying $\lambda^{(q)}(1; d) = 1$ [14]. This defines a *unique* value $\lambda^{(q)}(\alpha; d)$ and, from property (11), we have

$$\begin{aligned}\underbrace{\big(\mathcal{K}^{(q)}\big(\mathcal{K}^{(q)}\big(\cdots\big(\mathcal{K}^{(q)}\big(}_{k-d \text{ times}}\alpha^2\, T^{(q)}_{d}\big)\big)\big)\big)\big) &= T^{(q)}_k(\lambda^{(q)}(\alpha; d)) \\ &= T^{(q)}\, \frac{(1-\lambda^{(q)}(\alpha;d)\, x^{k-1})(1-\lambda^{(q)}(\alpha;d)\, x^{k+4})}{(1-\lambda^{(q)}(\alpha;d)\, x^{k+1})(1-\lambda^{(q)}(\alpha;d)\, x^{k+2})}\ .\end{aligned}$$

[14] As already noted, to be able to use property (11), we have to ensure that $\frac{(1-\lambda^2\, x^{2m+1})}{(1-\lambda\, x^m)(1-\lambda\, x^{m+1})}$ remains non-negative for $\lambda = \lambda^{(q)}(\alpha; d)$ and for all $m \le d+1$. Since x is in the range $0 \le x \le 1$, the most constraining requirement is for $m = d+1$, i.e. that $\frac{(1-\lambda^2\, x^{2d+3})}{(1-\lambda\, x^{d+1})(1-\lambda\, x^{d+2})} \ge 0$. Now this quantity changes sign upon changing $\lambda \to x^{-2d-3}/\lambda$, which precisely corresponds, in the equation for λ, to going from one branch of solution to the other. So only one of the solutions can be used, which by continuity is the branch satisfying $\lambda^{(q)}(1; d) = 1$ (the other branch satisfying $\lambda^{(q)}(1; d) = 1/x^{2d+3}$ is not acceptable).

By the same argument, we may compute the subtracted term in (13) and we find eventually that the generating function of k-slices with a weight $\alpha^{\mathcal{L}(d)}$ is given by

$$\begin{aligned} Z^{(q)}(\alpha;d,k) &= T_k^{(q)}(\lambda^{(q)}(\alpha;d)) - T_{k-1}^{(q)}(\lambda^{(q)}(\alpha;d-1)) \\ &= \frac{(1-x)(1-x^2)\left(1+4x+x^2\right)}{(1+x+x^2)}\times \\ &\times \frac{x^{k-1}(\lambda^{(q)}(\alpha;d-1)-\lambda^{(q)}(\alpha;d)\,x)\left(1-\lambda^{(q)}(\alpha;d-1)\lambda^{(q)}(\alpha;d)\,x^{2k+2}\right)}{\left(1-\lambda^{(q)}(\alpha;d-1)\,x^k\right)\left(1-\lambda^{(q)}(\alpha;d-1)\,x^{k+1}\right)\left(1-\lambda^{(q)}(\alpha;d)\,x^{k+1}\right)\left(1-\lambda^{(q)}(\alpha;d)\,x^{k+2}\right)} \end{aligned} \tag{15}$$

with $\lambda^{(q)}(\alpha;d)$ as in (14). This quantity is also the generating function of k-pointed-rooted quadrangulations as we defined them, with a fixed distance $d(v_0,v_1)=k\geq 3$, with a weight g per face and a weight $\alpha^{\mathcal{L}(d)}$ where $\mathcal{L}(d)$ is the hull perimeter at some fixed distance d ($2\leq d<k$) from v_0. The first terms of the expansion in g of $Z^{(q)}(\alpha;d,k)$ for the first allowed values of k and d are listed in Appendix B.

This calculation is trivially generalized to control simultaneously the perimeters at two distances d_1 and d_2 with $2\leq d_1\leq d_2<k$. We simply have to properly "insert" the weight α_1 at the d_1-th step of the recursion, then the weight α_2 at the d_2-th step. By doing so, we find that the generating function of k-pointed-rooted quadrangulations (with a fixed distance $d(v_0,v_1)=k\geq 3$) with a weight g per face and a weight $\alpha_1^{\mathcal{L}(d_1)}\alpha_2^{\mathcal{L}(d_2)}$ ($\mathcal{L}(d_1)$ and $\mathcal{L}(d_2)$ being the hull perimeters at respective distances d_1 and d_2 from v_0) is, for $d_1\leq d_2$:

$$Z^{(q)}(\alpha_1,\alpha_2;d_1,d_2)\equiv T_k^{(q)}(\lambda^{(q)}(\alpha_1,\alpha_2;d_1,d_2)) - T_{k-1}^{(q)}(\lambda^{(q)}(\alpha_1,\alpha_2;d_1-1,d_2-1))\ , \tag{16}$$

with $T_k^{(q)}(\lambda)$ as in (10), and where $\lambda^{(q)}(\alpha_1,\alpha_2;d_1,d_2)$ is defined as the solution of

$$\begin{aligned} &\frac{(1-\lambda^{(q)}(\alpha_1,\alpha_2;d_1,d_2)\,x^{d_2-1})(1-\lambda^{(q)}(\alpha_1,\alpha_2;d_1,d_2)\,x^{d_2+4})}{(1-\lambda^{(q)}(\alpha_1,\alpha_2;d_1,d_2)\,x^{d_2+1})(1-\lambda^{(q)}(\alpha_1,\alpha_2;d_1,d_2)\,x^{d_2+2})} \\ &\qquad = \alpha_2^2\,\frac{(1-\lambda^{(q)}(\alpha_1;d_1)\,x^{d_2-1})(1-\lambda^{(q)}(\alpha_1;d_1)\,x^{d_2+4})}{(1-\lambda^{(q)}(\alpha_1;d_1)\,x^{d_2+1})(1-\lambda^{(q)}(\alpha_1;d_1)\,x^{d_2+2})} \end{aligned} \tag{17}$$

with $\lambda^{(q)}(\alpha_1;d_1)$ defined as in (14). Again the equation is quadratic in $\lambda^{(q)}(\alpha_1,\alpha_2;d_1,d_2)$ and we pick the branch of solution satisfying $\lambda^{(q)}(\alpha_1,1;d_1,d_2)=\lambda^{(q)}(\alpha_1;d_1)$.

3.2. **The case of triangulations.**

3.2.1. *The slice recursion.* Let us now discuss k-slices, as defined in Section 2.1 in correspondence with k-pointed-rooted triangulations. Again we consider the larger set of ℓ-slices with $1\leq\ell\leq k$ and denote by $R_k^{(t)}\equiv R_k^{(t)}(g)$, $k\geq 1$ their generating function with a weight g per inner triangle. The function $R_k^{(t)}$ is also the generating function of pointed-rooted triangulations with $1\leq d(v_0,v_1)\leq k$ and a weight g per triangle[15]. The explicit expression for $R_k^{(t)}$ reads [5]:

$$R_k^{(t)} = R^{(t)}\frac{(1-x^k)(1-x^{k+2})}{(1-x^{k+1})^2}\ , \qquad R^{(t)}=\frac{\sqrt{1+10x+x^2}}{1+x}\ .$$

where x parametrizes g through

$$g=\frac{\sqrt{x(1+x)}}{(1+10x+x^2)^{3/4}}\ .$$

Again we fix x univocally by imposing the extra condition $0\leq x\leq 1$: the generating functions are now well-defined for real g in the range $0\leq g\leq 1/(2\cdot 3^{3/4})$. The recursion relation involves, in addition to $R_k^{(t)}$, the generating function $T_k^{(t)}$ of ℓ-*isoslices* with $1\leq\ell\leq k$

[15]By pointed-rooted triangulations, we mean in general ℓ-pointed-rooted triangulations with arbitrary $\ell\geq 1$. In particular, the endpoint of the marked edge e_1 is at distance 1 less from the origin than its first extremity.

and a weight g per inner triangle. The ℓ-isoslices are defined exactly as ℓ-slices except that both their right and left boundaries have the same length ℓ (in other fords, both extremities of the base are at distance ℓ from the apex – see figure 14). Note that, as opposed to ℓ-slices, ℓ-isoslices are not related bijectively to some particular set of triangulations. We have the explicit expression [5]:

$$T_k^{(t)} = T^{(t)} \frac{(1-x^k)(1-x^{k+3})}{(1-x^{k+1})(1-x^{k+2})} , \qquad T^{(t)} = \sqrt{x}\, \frac{(1+10x+x^2)^{1/4}}{(1+x)^{3/2}} .$$

The recursion relation of [5], which fixes $R_k^{(t)}$ and $T_k^{(t)}$, may now be written as:

$$\begin{aligned} & R_k^{(t)} = \mathcal{N}^{(t)}(T_{k-1}^{(t)}) \qquad T_k^{(t)} = \mathcal{K}^{(t)}(T_{k-1}^{(t)}) , \\ & \mathcal{N}^{(t)}(T) = \frac{R_1^{(t)}}{1 - R_1^{(t)}\, T\, \Phi^{(t)}(T)} , \\ & \mathcal{K}^{(t)}(T) = \frac{(R_1^{(t)})^2}{1 - R_1^{(q)}\, T\, \Phi^{(t)}(T)} , \qquad \Phi^{(t)}(T) \equiv \Phi^{(t)}(T,g) = \sum_{i\geq 3} h_i^{(t)}(g)\, T^{i-3} , \end{aligned} \tag{18}$$

for $k \geq 1$ with $T_0^{(t)} = 0$. Here the quantities $h_i^{(t)}(g)$ denote appropriate generating functions defined in [5] and whose explicit expression is not needed. Again we note that the kernels $\mathcal{N}^{(t)}(T)$ and $\mathcal{K}^{(t)}(T)$ are independent of k while $R_k^{(t)}$ and $T_k^{(t)}$ depend on k only through the variable x^k. A before, we immediately deduce that, if we set

$$R_k^{(t)}(\lambda) = R^{(t)} \frac{(1-\lambda\, x^k)(1-\lambda\, x^{k+2})}{(1-\lambda\, x^{k+1})^2} , \qquad T_k^{(t)}(\lambda) = T^{(t)} \frac{(1-\lambda\, x^k)(1-\lambda\, x^{k+3})}{(1-\lambda\, x^{k+1})(1-\lambda\, x^{k+2})} , \tag{19}$$

then

$$R_k^{(t)}(\lambda) = \mathcal{N}^{(t)}(T_{k-1}^{(t)}(\lambda)) , \qquad T_k^{(t)}(\lambda) = \mathcal{K}^{(t)}(T_{k-1}^{(t)}(\lambda)) \tag{20}$$

(for λ close enough to 1).

3.2.2. *Controlling the hull perimeter.* Again the recursion relation is intimately linked to the notion of hull perimeter. Let us recall how it works for triangulations. We consider an ℓ-isoslice with left boundary length ℓ between 1 and k (as enumerated by $T_k^{(t)}$) and cut it along its so-called dividing line (as defined in [5]) which is nothing but the hull boundary at distance $\ell - 1$ from v_0 in the ℓ-isoslice, defined exactly as in Section 2.1 (see figure 14 for an illustration)[16]. Thanks to this cutting, we deduce that the generating function $T_k^{(t)}$ is the product of the generating function of the domain $\mathcal{C}_{\ell-1}$ times that of the domain $\mathcal{H}_{\ell-1}$. For a fixed value $\mathcal{L}$ of the hull perimeter $\mathcal{L}(\ell-1)$, the first generating function is simply:

$$[T^{\mathcal{L}}]\mathcal{K}^{(t)}(T)$$

while the second generating function reads:

$$\left(T_{k-1}^{(t)}\right)^{\mathcal{L}} .$$

This is because the domain $\mathcal{H}_{\ell-1}$ may be decomposed into exactly $\mathcal{L}$ sub-isoslices with left boundary lengths ℓ_i, $1 \leq i \leq \mathcal{L}$, satisfying $1 \leq \ell_i \leq \ell - 1$, hence $1 \leq \ell_i \leq k-1$ when considering all possible values of ℓ. As before, these sub-isoslices are obtained by cutting along the leftmost shortest paths to v_0 from the $\mathcal{L}-1$ internal vertices of the hull boundary at distance $\ell - 1$. Each of the $\mathcal{L}$ sub-isoslices contributes a factor $T_{k-1}^{(t)}$ to the generating function. Summing over all values of $\mathcal{L}$ yields the desired recursion relation (18). To assign a weight $\alpha^{\mathcal{L}}$ to our ℓ-isoslices, we simply need to replace $T_{k-1}^{(t)}$ by $\alpha\, T_{k-1}^{(t)}$ at the step $k-1 \to k$

[16]When $\ell = 1$, the hull boundary at distance $\ell - 1 = 0$ must be understood as reduced to the single vertex v_0, having length 0.

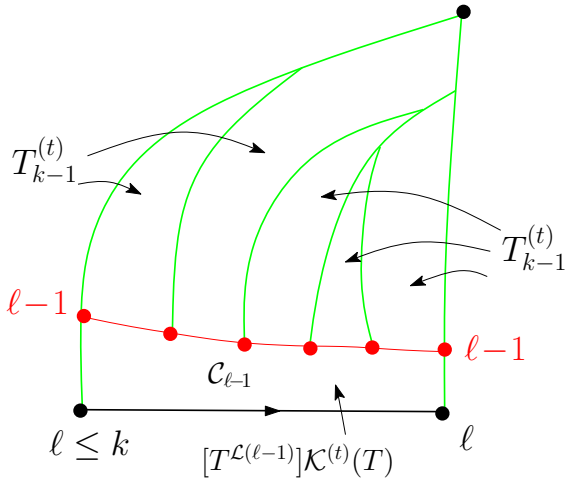

FIGURE 14. Schematic representation of an ℓ-isoslice and its decomposition by cutting along the hull boundary at distance $\ell-1$ from its apex. The domain $\mathcal{C}_{\ell-1}$ is enumerated by $[T^{\mathcal{L}}]\mathcal{K}^{(t)}(T)$ if the value of the hull perimeter $\mathcal{L}(\ell-1)$ is $\mathcal{L}$ while the complementary domain is formed of $\mathcal{L}$ isoslices, each enumerated by $T_{k-1}^{(t)}$ (if we wish, for fixed $\mathcal{L}$, to count all the ℓ-isoslices satisfying $1 \le \ell \le k$). Here $\mathcal{L}=5$.

of the recursion so that the generating function of ℓ-isoslices with $1 \le \ell \le k$, with a weight g per inner face and a weight $\alpha^{\mathcal{L}(\ell-1)}$ is simply

$$\mathcal{K}^{(t)}(\alpha\, T_{k-1}^{(t)})$$

(again, ℓ-isoslices with $\ell=1$ must be understood as having $\mathcal{L}(\ell-1)=0$, hence are enumerated with a weight $\alpha^{\mathcal{L}(\ell-1)}=1$).

As for the relation giving $R_k^{(t)}$ in (18), it follows from a similar decomposition of ℓ-slices with left boundary length ℓ between 1 and k. The hull $\mathcal{H}_{\ell-1}$ is characterized by exactly the same distance constraints as for isoslices, hence yields the same generating function $\left(T_{k-1}^{(t)}\right)^{\mathcal{L}}$ if $\mathcal{L}(\ell-1)$ has a fixed value $\mathcal{L}$. Only the domain $\mathcal{C}_{\ell-1}$ is modified and has then generating function $[T^{\mathcal{L}}]\mathcal{N}^{(t)}(T)$ (see figure 15). This leads to the desired relation in (18). Again, we may easily assign a weight $\alpha^{\mathcal{L}}$ by multiplying $T_{k-1}^{(t)}$ by α. In other words, the generating function of ℓ-slices with $1 \le \ell \le k$, with a weight g per inner face and a weight $\alpha^{\mathcal{L}(\ell-1)}$ is

$$\mathcal{N}^{(t)}(\alpha\, T_{k-1}^{(t)})$$

(ℓ-slices with $\ell=1$ are enumerated with a weight $\alpha^{\mathcal{L}(\ell-1)}=1$).

Repeating the argument of Section 3.1, we obtain, for $1 \le m < k$, the generating functions of, respectively, ℓ-slices and ℓ-isoslices with $1 \le \ell \le k$ with a weight g per inner face and a weight $\alpha^{\mathcal{L}(\ell-m)}$ whenever $\ell \ge m$, namely:

$$\begin{aligned} &\mathcal{N}^{(t)}\big(\underbrace{\mathcal{K}^{(t)}\big(\cdots\big(\mathcal{K}^{(t)}\big(}_{m-1 \text{ times}}\alpha\, T_{k-m}^{(t)}\big)\big)\big)\big) \qquad \text{and} \\ &\underbrace{\mathcal{K}^{(t)}\big(\mathcal{K}^{(t)}\big(\cdots\big(\mathcal{K}^{(t)}\big(}_{m \text{ times}}\alpha\, T_{k-m}^{(t)}\big)\big)\big)\big) \qquad \text{respectively} \end{aligned} \tag{21}$$

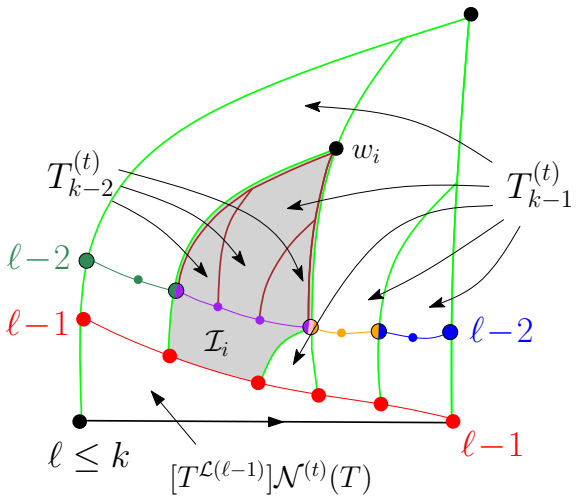

FIGURE 15. Schematic representation of an ℓ-slice and its decomposition by cutting along the hull boundary at distance $\ell-1$ from its apex. The domain below the hull boundary is now enumerated by $[T^{\mathcal{L}}]\mathcal{N}^{(t)}(T)$ if the value of the hull perimeter $\mathcal{L}(\ell-1)$ is $\mathcal{L}$ while the complementary domain is formed of $\mathcal{L}$ isoslices $\mathcal{I}_i$ of left boundary length ℓ_i, exactly as in figure 14, each enumerated by $T^{(t)}_{k-1}$ (if we wish, for fixed $\mathcal{L}$, to enumerate all ℓ-slices with $1 \le \ell \le k$). The hull boundary at distance $\ell-2$ from the apex is obtained by concatenating the hull boundaries at distance $\ell_i - 1$ from their apex w_i of all the sub-isoslices $\mathcal{I}_i$.

(see figure 15 for an illustration of the first identity when $m=2$).

If we now take $k \ge 2$ and d in the range $1 \le d \le k-1$, the generating function of k-slices with a weight g per inner face and a weight $\alpha^{\mathcal{L}(d)}$ is

$$\mathcal{N}^{(t)}\big(\underbrace{\mathcal{K}^{(t)}\big(\cdots\big(\mathcal{K}^{(t)}\big(}_{k-d-1 \text{ times}}\alpha\, T^{(t)}_d\big)\big)\big)\big) - \mathcal{N}^{(t)}\big(\underbrace{\mathcal{K}^{(t)}\big(\cdots\big(\mathcal{K}^{(t)}\big(}_{k-d-1\text{times}}\alpha\, T^{(t)}_{d-1}\big)\big)\big)\big)\ .$$

As for quadrangulations, both terms in the equation may be computed upon defining $\lambda^{(t)}(\alpha;d)$ as the solution of the equation

$$T^{(t)}_d(\lambda^{(t)}(\alpha;d)) = \alpha\, T^{(t)}_d\ ,$$

namely

$$\frac{(1-\lambda^{(t)}(\alpha;d)\,x^d)(1-\lambda^{(t)}(\alpha;d)\,x^{d+3})}{(1-\lambda^{(t)}(\alpha;d)\,x^{d+1})(1-\lambda^{(t)}(\alpha;d)\,x^{d+2})} = \alpha\,\frac{(1-x^d)(1-x^{d+3})}{(1-x^{d+1})(1-x^{d+2})} \tag{22}$$

where we pick the branch of solution satisfying $\lambda^{(t)}(1;d)=1$. From property (20), we have

$$\begin{aligned}\mathcal{N}^{(t)}\big(\underbrace{\mathcal{K}^{(t)}\big(\cdots\big(\mathcal{K}^{(t)}\big(}_{k-d-1 \text{ times}}\alpha\, T^{(q)}_d\big)\big)\big)\big) &= R^{(t)}_k(\lambda^{(t)}(\alpha;d)) \\ &= R^{(t)}\,\frac{(1-\lambda^{(t)}(\alpha;d)\,x^k)(1-\lambda^{(t)}(\alpha;d)\,x^{k+2})}{(1-\lambda^{(t)}(\alpha;d)\,x^{k+1})^2}\ .\end{aligned}$$

so that the generating function of k-slices with a weight $\alpha^{\mathcal{L}(d)}$ eventualy reads

$$\begin{aligned} Z^{(t)}(\alpha;d,k) &= R_k^{(t)}(\lambda^{(t)}(\alpha;d)) - R_{k-1}^{(t)}(\lambda^{(t)}(\alpha;d-1)) \\ &= \frac{(1-x)^2\sqrt{1+10x+x^2}}{(1+x)}\times \\ &\quad\times \frac{x^{k-1}(\lambda^{(t)}(\alpha;d-1)-\lambda^{(t)}(\alpha;d)\,x)\left(1-\lambda^{(t)}(\alpha;d-1)\lambda^{(t)}(\alpha;d)\,x^{2k+1}\right)}{\left(1-\lambda^{(t)}(\alpha;d-1)\,x^k\right)^2\left(1-\lambda^{(t)}(\alpha;d)\,x^{k+1}\right)^2} \end{aligned} \tag{23}$$

with $\lambda^{(t)}(\alpha;d)$ as in (22). This is also the generating function of k-pointed-rooted triangulations as we defined them, with a fixed distance $d(v_0,v_1)=k\geq 2$, with a weight g per triangle and a weight $\alpha^{\mathcal{L}(d)}$ where $\mathcal{L}(d)$ is the hull perimeter at some fixed distance d ($1\leq d<k$) from v_0. The first terms of the expansion in g of $Z^{(t)}(\alpha;d,k)$ for the first allowed values of k and d are listed in Appendix B.

Again we may impose a simultaneous control on the perimeters at two distances d_1 and d_2 ($1\leq d_1\leq d_2<k$). The generating function of k-pointed-rooted triangulations (with a fixed distance $d(v_0,v_1)=k\geq 2$) with a weight g per face and a weight $\alpha_1^{\mathcal{L}(d_1)}\alpha_2^{\mathcal{L}(d_2)}$ ($\mathcal{L}(d_1)$ and $\mathcal{L}(d_2)$ being the hull perimeters at respective distances d_1 and d_2 from v_0) is, for $d_1\leq d_2$:

$$Z^{(t)}(\alpha_1,\alpha_2;d_1,d_2) \equiv R_k^{(t)}(\lambda^{(t)}(\alpha_1,\alpha_2;d_1,d_2)) - R_{k-1}^{(t)}(\lambda^{(t)}(\alpha_1,\alpha_2;d_1-1,d_2-1))\ , \tag{24}$$

with $R_k^{(t)}(\lambda)$ as in (19), and where $\lambda^{(t)}(\alpha_1,\alpha_2;d_1,d_2)$ is defined as the solution of

$$\begin{aligned} &\frac{(1-\lambda^{(t)}(\alpha_1,\alpha_2;d_1,d_2)\,x^{d_2})(1-\lambda^{(t)}(\alpha_1,\alpha_2;d_1,d_2)\,x^{d_2+3})}{(1-\lambda^{(t)}(\alpha_1,\alpha_2;d_1,d_2)\,x^{d_2+1})(1-\lambda^{(t)}(\alpha_1,\alpha_2;d_1,d_2)\,x^{d_2+2})} \\ &\qquad = \alpha_2\,\frac{(1-\lambda^{(t)}(\alpha_1;d_1)\,x^{d_2})(1-\lambda^{(t)}(\alpha_1;d_1)\,x^{d_2+3})}{(1-\lambda^{(t)}(\alpha_1;d_1)\,x^{d_2+1})(1-\lambda^{(t)}(\alpha_1;d_1)\,x^{d_2+2})} \end{aligned} \tag{25}$$

with $\lambda^{(t)}(\alpha_1;d_1)$ defined as in (22). The correct branch of solutions for $\lambda^{(t)}(\alpha_1,\alpha_2;d_1,d_2)$ is that satisfying $\lambda^{(t)}(\alpha_1,1;d_1,d_2)=\lambda^{(t)}(\alpha_1;d_1)$.

4. The limit of large maps

4.1. **Singularity analysis.** We now have at our disposal all the required generating functions. Let us recall how to extract from these quantities the desired expectation values and probability distributions. Our results of Section 2.2 apply to the ensemble of uniformly drawn k-pointed-rooted quadrangulations (respectively triangulations) having a fixed number N of faces and a fixed value k of the distance between their origin v_0 and the first extremity v_1 of their marked edge e_1. In our generating functions, k is already fixed but, in order to have a fixed N, we must in principle extract the coefficient of g^N in their expansion in g. In Section 2.2, we specialized our results to the limit $N\to\infty$: the asymptotic behavior of the coefficient of g^N is then directly encoded in the singular behavior of the generating functions. In the case of quadrangulations, a singularity occurs when g approaches its "critical value" $1/12$, corresponding to the limit $x\to 1$. For triangulations, the singularity is for $g\to 1/(2\cdot 3^{3/4})$. The singular behavior is best captured by setting

$$\begin{aligned} g &= \frac{1}{12}\left(1-\epsilon^4\right) \qquad \text{for quadrangulations}\ , \\ g &= \frac{1}{2\cdot 3^{3/4}}\left(1-\epsilon^4\right) \qquad \text{for triangulations}\ , \end{aligned}$$

and expanding our various generating functions around $\epsilon=0$.

Let us now discuss in details the case of quadrangulations. The small ϵ expansion of $Z^{(q)}(\alpha;d,k)$ takes the form:

$$Z^{(q)}(\alpha;d,k) = A_0^{(q)}(\alpha;d,k) + A_2^{(q)}(\alpha;d,k)\epsilon^4 + A_3^{(q)}(\alpha;d,k)\epsilon^6 + O(\epsilon^8)\ , \tag{26}$$

where we note in particular *the absence of a term of order* ϵ^2. The constant term and the term of order $\epsilon^4 = 1 - 12\,g$ being regular, the most singular part of $Z^{(q)}(\alpha; d, k)$ is therefore

$$Z^{(q)}(\alpha; d, k)|_{\text{sing.}} = A_3^{(q)}(\alpha; d, k)\ (1 - 12\,g)^{3/2}$$

and, by a standard result, we deduce the large N behavior

$$[g^N]Z^{(q)}(\alpha; d, k) \sim \frac{3}{4}\ \frac{12^N}{N^{5/2}} \times A_3^{(q)}(\alpha; d, k)\ .$$

This gives the large N asymptotics of the "reduced" generating function (with α as only left variable) of k-pointed-rooted quadrangulations with a fixed number N of faces, a fixed distance $d(v_0, v_1) = k$ and a weight $\alpha^{\mathcal{L}(d)}$. To get the expectation value of $\alpha^{\mathcal{L}(d)}$ in the ensemble of k-pointed-rooted quadrangulations with fixed N and k, we must divide this generating function by the cardinal of this ensemble. The latter is easily obtained by taking $\alpha = 1$, in which case $Z^{(q)}(\alpha; d, k)$ and $A_3^{(q)}(\alpha; d, k)$ do not depend on d (recall that $\lambda(1; d) = 1$ independently of d). The large N behavior of the *number* of k-pointed-rooted quadrangulations with fixed N and k is thus

$$[g^N]Z^{(q)}(1; d, k) \sim \frac{3}{4}\ \frac{12^N}{N^{5/2}} \times A_3^{(q)}(1; d, k)$$

irrespectively of d. The expectation value of $\alpha^{\mathcal{L}(d)}$ in our ensemble is thus simply

$$W_k^{(q)}(\alpha; d) \equiv E_k(\alpha^{\mathcal{L}(d)}) = \frac{A_3^{(q)}(\alpha; d, k)}{A_3^{(q)}(1; d, k)}\ . \tag{27}$$

The computation of $W_k^{(q)}(\alpha; d)$, although straightforward, is quite cumbersome and we do not give its full expression here. As we discussed in Section 2.2, our main interest is the limit of large k. If we send $k \to \infty$, *keeping d finite*, the expression of $W_k^{(q)}(\alpha; d)$ drastically simplifies and we find

$$\begin{aligned} W_\infty^{(q)}(\alpha; d) = \frac{1}{2}\Bigg(& -\frac{\sqrt{(d-2)^2(d+3)^2\alpha^4 - 26(d-2)d(d+1)(d+3)\alpha^2 + 25d^2(d+1)^2}}{d(d+1)\,(1-\alpha^2) + 6\alpha^2} \\ & + \frac{\sqrt{(d-1)^2(d+4)^2\alpha^4 - 26(d-1)(d+1)(d+2)(d+4)\alpha^2 + 25(d+1)^2(d+2)^2}}{(d+1)(d+2)\,(1-\alpha^2) + 6\alpha^2}\Bigg)\ . \end{aligned} \tag{28}$$

In particular, the average length $\mathcal{L}(d)$ is simply

$$E_\infty(\mathcal{L}(d)) = \frac{\partial}{\partial\alpha} W_\infty^{(q)}(\alpha; d)|_{\alpha=1} = \frac{2(d+1)^2\left(3d^2 + 6d - 4\right)}{3(2d+1)(2d+3)}\ .$$

For large d, this average length scales like $d^2/2 = (3c/2) \times d^2$ with $c = 1/3$. Introducing as in Section 2.2 the rescaled variable $L(d) \equiv \mathcal{L}(d)/d^2$, we have

$$\lim_{d\to\infty} E_\infty(e^{-\tau L(d)}) = \lim_{d\to\infty} W_\infty^{(q)}(e^{-\frac{\tau}{d^2}}; d) = \frac{1}{(1 + c\,\tau)^{3/2}}$$

with $c = 1/3$, as announced in eq. (1).

Returning to a finite value of k, we give in Appendix C the general expression for the average length $\mathcal{L}(d)$, i.e. the expression of

$$E_k(\mathcal{L}(d)) = \frac{\partial}{\partial\alpha} W_k^{(q)}(\alpha; d)|_{\alpha=1}\ .$$

From this expression, we deduce, by considering the limit of both d and k large, with a fixed value of the ratio $u = d/k$ $(0 < u < 1)$, the average value $L_{\text{av}}(u)$ of rescaled length $L(d)$, namely:

$$L_{\text{av}}(u) \equiv \lim_{k\to\infty} \frac{1}{(k\,u)^2} E_k(\mathcal{L}(k\,u)) = \frac{3c}{2}(1 + u - 3u^6 + u^7)$$

with $c = 1/3$, as announced in Section 2.2.

We may perform similar calculations for triangulations, taking as starting point the quantity $Z^{(t)}(\alpha; d, k)$ of eq. (23). Following the same lines as above, we obtain an expression for

$$W_k^{(t)}(\alpha; d) \equiv E_k(\alpha^{\mathcal{L}(d)})$$

in the ensemble of k-pointed-rooted triangulations with fixed k and N, in the asymptotic limit where $N \to \infty$. In particular, we now get

$$W_\infty^{(t)}(\alpha; d) = \frac{1}{2}\left(-\frac{\sqrt{(d-1)(d+2)((d-1)(d+2)(9-\alpha)(1-\alpha) - 20\alpha + 36) + 36}}{(d-1)(d+2)(1-\alpha)+2} + \frac{\sqrt{d(d+3)(d(d+3)(9-\alpha)(1-\alpha) - 20\alpha + 36) + 36}}{d(d+3)(1-\alpha)+2} \right), \tag{29}$$

from which we extract

$$E_\infty(\mathcal{L}(d)) = \frac{3d(d+1)^2(d+2)}{(2d+1)(2d+3)},$$

which now scales at large d as $3d^2/4 = (3c/2) \times d^2$ with $c = 1/2$. The explicit formula of $E_k(\mathcal{L}(d))$ for finite k and d is presented in Appendix C. We also easily compute as above the values of $\lim_{d\to\infty} E_\infty(e^{-\tau L(d)})$ and $L_{\rm av}(u)$ for triangulations, whose expressions are exactly the same as for quadrangulations, except for the value of c, now equal to $1/2$.

4.2. **A shortcut in the calculations.** The calculations above were performed for finite d and k, leading to some non-universal quantities with rather involved expressions from which we then extracted some of the universal laws at $d, k \to \infty$ announced in Section 2.2, such as the expressions for $L_{\rm av}(u)$ and for $\lim_{d\to\infty} E_\infty(e^{-\tau L(d)})$. To obtain in a more systematic way the results of Section 2.2, we may simplify our calculations and incorporate *ab initio* the fact that k and d are eventually supposed to be large.

4.2.1. *A more direct computation of the probability density for $L(d)$ when $k \to \infty$.* We start again with the case of quadrangulations. All our calculations rely on the expression of $A_3^{(q)}(\alpha; d, k)$ in (26). The large k behavior of this coefficient may be deduced from the so-called *scaling limit* where we let $\epsilon \to 0$ and $k \to \infty$ as

$$k = \frac{K}{\epsilon}$$

with K finite. More precisely, when $\epsilon \to 0$, we have the expansions

$$x = 1 - \sqrt{6}\,\epsilon + O(\epsilon^2)$$
$$\lambda^{(q)}(\alpha; d) = 1 - \Lambda^{(q)}(\alpha; d)\epsilon + O(\epsilon^2)$$

where $\Lambda^{(q)}(\alpha; d)$ is obtained by expanding (14) at leading order in ϵ, namely as the solution of

$$\frac{\left(\Lambda^{(q)}(\alpha; d)\right)^2 + \sqrt{6}(2d+3)\Lambda^{(q)}(\alpha; d) + 6(d-1)(d+4)}{\left(\Lambda^{(q)}(\alpha; d)\right)^2 + \sqrt{6}(2d+3)\Lambda^{(q)}(\alpha; d) + 6(d+1)(d+2)} = \alpha^2 \frac{(d-1)(d+4)}{(d+1)(d+2)} \tag{30}$$

which vanishes when $\alpha = 1$. We then have the scaling behavior when $\epsilon \to 0$:

$$Z^{(q)}\left(\alpha; d, \frac{K}{\epsilon}\right) \sim \mathcal{Z}^{(q)}(\alpha; d, K)\,\epsilon^3$$

$$\mathcal{Z}^{(q)}(\alpha; d, K) = \left(\frac{24 e^{\sqrt{6}K}\left(1 + e^{\sqrt{6}K}\right)\left(\Lambda^{(q)}(\alpha; d) - \Lambda^{(q)}(\alpha; d-1) + \sqrt{6}\right)}{\left(e^{\sqrt{6}K} - 1\right)^3} \right).$$

To be consistent with the expansion (26), the coefficient $A_i^{(q)}(\alpha;d,k)$ must behave at large k as k^{2i-3} and more precisely

$$A_i^{(q)}(\alpha;d,k) \underset{k\to\infty}{\sim} k^{2i-3} \times [K^{2i-3}]\mathcal{Z}^{(q)}(\alpha;d,K)\ .$$

Expanding $\mathcal{Z}^{(q)}(\alpha;d,K)$ at small K and extracting the term of order K^3, we thus deduce

$$A_3^{(q)}(\alpha;d,k) \underset{k\to\infty}{\sim} k^3 \times \frac{2}{7}\sqrt{\frac{2}{3}}\left(\Lambda^{(q)}(\alpha;d)-\Lambda^{(q)}(\alpha;d-1)+\sqrt{6}\right)$$

and, from (27),

$$E_k(\alpha^{\mathcal{L}(d)}) = W_k^{(q)}(\alpha;d) \underset{k\to\infty}{\sim} \frac{\Lambda^{(q)}(\alpha;d)-\Lambda^{(q)}(\alpha;d-1)+\sqrt{6}}{\sqrt{6}} \tag{31}$$

from which (28) follows immediately. When $d\to\infty$, we easily get from (30) that

$$\Lambda^{(q)}(e^{-\frac{\tau}{d^2}};d) = \sqrt{6}\,d\left(\frac{1}{\sqrt{1+c\,\tau}}-1\right)+3\sqrt{\frac{3}{2}}\left(\frac{1}{(1+c\,\tau)^{3/2}}-1\right)+O\left(\frac{1}{d}\right)$$

$$\Lambda^{(q)}(e^{-\frac{\tau}{d^2}};d-1) = \sqrt{6}\,d\left(\frac{1}{\sqrt{1+c\,\tau}}-1\right)+\sqrt{\frac{3}{2}}\left(\frac{1}{(1+c\,\tau)^{3/2}}-1\right)+O\left(\frac{1}{d}\right)$$

with $c=1/3$ and (31) immediately implies (1) and, by some inverse Laplace transform, the expression (2) of the probability density for $L(d)$ when d is large. In conclusion, the above approach based on the scaling limit provides a more direct proof of our first main result, here for quadrangulations.

4.2.2. *Computation of the joint probability density for $L(d_1)$ and $L(d_2)$ when $k\to\infty$.* By a straightforward extension of the above analysis, we find that, for $d_1\le d_2$,

$$E_k(\alpha_1^{\mathcal{L}(d_1)}\alpha_2^{\mathcal{L}(d_2)}) \underset{k\to\infty}{\sim} \frac{\Lambda^{(q)}(\alpha_1,\alpha_2;d_1,d_2)-\Lambda^{(q)}(\alpha_1,\alpha_2;d_1-1,d_2-1)+\sqrt{6}}{\sqrt{6}} \tag{32}$$

where $\Lambda^{(q)}(\alpha_1,\alpha_2;d_1,d_2)$ is fixed by

$$\frac{\left(\Lambda^{(q)}(\alpha_1,\alpha_2;d_1,d_2)\right)^2+\sqrt{6}(2d_2+3)\Lambda^{(q)}(\alpha_1,\alpha_2;d_1,d_2)+6(d_2-1)(d_2+4)}{\left(\Lambda^{(q)}(\alpha_1,\alpha_2;d_1,d_2)\right)^2+\sqrt{6}(2d_2+3)\Lambda^{(q)}(\alpha_1,\alpha_2;d_1,d_2)+6(d_2+1)(d_2+2)} =$$
$$\alpha_2^2\,\frac{\left(\Lambda^{(q)}(\alpha_1;d_1)\right)^2+\sqrt{6}(2d_2+3)\Lambda^{(q)}(\alpha_1;d_1)+6(d_2-1)(d_2+4)}{\left(\Lambda^{(q)}(\alpha_1;d_1)\right)^2+\sqrt{6}(2d_2+3)\Lambda^{(q)}(\alpha_1;d_1)+6(d_2+1)(d_2+2)}$$

with $\Lambda^{(q)}(\alpha_1;d_1)$ defined by (30) (we pick the solution such that $\Lambda^{(q)}(\alpha_1,1;d_1,d_2)=\Lambda^{(q)}(\alpha_1;d_1)$). Setting $d_1=d$, $d_2=v\,d$ ($v\ge1$) and letting $d\to\infty$, we then have

$$\Lambda^{(q)}(e^{-\frac{\tau_1}{d^2}},e^{-\frac{\tau_2}{(v\,d)^2}};d,v\,d) = \sqrt{6}\,d\,v\left(\frac{1+(v-1)\omega_1}{\sqrt{v^2\,\omega_1^2+c\,\tau_2(1+(v-1)\omega_1)^2}}-1\right)$$
$$+3\sqrt{\frac{3}{2}}\left(\frac{v^3}{(v^2\,\omega_1^2+c\,\tau_2(1+(v-1)\omega_1)^2)^{3/2}}-1\right)+O\left(\frac{1}{d}\right)$$

$$\Lambda^{(q)}(e^{-\frac{\tau_1}{d^2}},e^{-\frac{\tau_2}{(v\,d)^2}};d-1,v\,d-1) = \sqrt{6}\,d\,v\left(\frac{1+(v-1)\omega_1}{\sqrt{v^2\,\omega_1^2+c\,\tau_2(1+(v-1)\omega_1)^2}}-1\right)$$
$$+\sqrt{\frac{3}{2}}\left(\frac{v^3}{(v^2\,\omega_1^2+c\,\tau_2(1+(v-1)\omega_1)^2)^{3/2}}-1\right))+O\left(\frac{1}{d}\right)$$

where $\omega_1\equiv\sqrt{1+c\,\tau_1}$,

with $c=1/3$. Plugging these expansions in (32), we deduce the announced result (6). Knowing (6), it is not difficult to deduce the expression (7) for the joint probability density

$\mathcal{P}(L_1,L_2;v)$ by performing a double inverse Laplace transform. The details of this transformation are presented in Appendix A. This proves our third main result for quadrangulations.

4.2.3. *Similar results for triangulations.* In the case of triangulations, we find along the same lines

$$E_k(\alpha^{\mathcal{L}(d)}) = W_k^{(t)}(\alpha;d) \underset{k\to\infty}{\sim} \frac{\Lambda^{(t)}(\alpha;d)-\Lambda^{(t)}(\alpha;d-1)+\sqrt{8\sqrt{3}}}{\sqrt{8\sqrt{3}}} \tag{33}$$

with $\Lambda^{(t)}(\alpha;d)$ fixed by

$$\frac{\left(\Lambda^{(t)}(\alpha;d)\right)^2+\sqrt{8\sqrt{3}}(2d+3)\Lambda^{(t)}(\alpha;d)+8\sqrt{3}\,d(d+3)}{\left(\Lambda^{(t)}(\alpha;d)\right)^2+\sqrt{8\sqrt{3}}(2d+3)\Lambda^{(t)}(\alpha;d)+8\sqrt{3}(d+1)(d+2)} = \alpha\,\frac{d\,(d+3)}{(d+1)(d+2)}\ .$$

This immediately leads to (29) for finite d and, in the limit $d\to\infty$, to (1) with $c=1/2$. We have similarly

$$E_k(\alpha_1^{\mathcal{L}(d_1)}\alpha_2^{\mathcal{L}(d_2)}) \underset{k\to\infty}{\sim} \frac{\Lambda^{(t)}(\alpha_1,\alpha_2;d_1,d_2)-\Lambda^{(t)}(\alpha_1,\alpha_2;d_1-1,d_2-1)+\sqrt{8\sqrt{3}}}{\sqrt{8\sqrt{3}}}$$

with $\Lambda^{(t)}(\alpha_1,\alpha_2;d_1,d_2)$ now fixed by

$$\frac{\left(\Lambda^{(t)}(\alpha_1,\alpha_2;d_1,d_2)\right)^2+\sqrt{8\sqrt{3}}(2d_2+3)\Lambda^{(t)}(\alpha_1,\alpha_2;d_1,d_2)+8\sqrt{3}\,d_2(d_2+3)}{\left(\Lambda^{(t)}(\alpha_1,\alpha_2;d_1,d_2)\right)^2+\sqrt{8\sqrt{3}}(2d_2+3)\Lambda^{(t)}(\alpha_1,\alpha_2;d_1,d_2)+8\sqrt{3}(d_2+1)(d_2+2)} =$$
$$\alpha_2\,\frac{\left(\Lambda^{(t)}(\alpha_1;d_1)\right)^2+\sqrt{8\sqrt{3}}(2d_2+3)\Lambda^{(t)}(\alpha_1;d_1)+8\sqrt{3}\,d_2(d_2+3)}{\left(\Lambda^{(t)}(\alpha_1;d_1)\right)^2+\sqrt{8\sqrt{3}}(2d_2+3)\Lambda^{(t)}(\alpha_1;d_1)+8\sqrt{3}(d_2+1)(d_2+2)}\ .$$

Setting $d_1=d$, $d_2=v\,d$ and sending $d\to\infty$ leads again to (6), now with $c=1/2$. This ends the proof of our first and third main results for triangulations.

4.3. **The hull perimeter at a finite fraction of the total distance.** We end our calculation with the derivation of (4), corresponding to the limit $d,k\to\infty$ with $u=d/k$ fixed ($0<u<1$). For quadrangulations, we have

$$\lim_{k\to\infty} E_k(e^{-\tau L(k\,u)}) = \lim_{k\to\infty} W_k^{(q)}(e^{-\frac{\tau}{(k\,u)^2}};k\,u) = \lim_{k\to\infty}\frac{A_3^{(q)}(e^{-\frac{\tau}{(k\,u)^2}};k\,u,k)}{A_3^{(q)}(1;k\,u,k)}$$

(recall that the denominator in the last expression is actually independent of u). Again the full knowledge of $A_3^{(q)}(\alpha;d,k)$ is not required to handle the limit of large k and we may again have recourse to the scaling limit by setting $k=K/\epsilon$ and letting $\epsilon\to 0$. We have now the expansions

$$\begin{aligned}&\lambda^{(q)}\left(e^{-\frac{\tau}{(K\,u)^2}\epsilon^2};\frac{K\,u}{\epsilon}\right) = \mu^{(q)}-\nu^{(q)}\epsilon+O(\epsilon^2)\\ &\lambda^{(q)}\left(e^{-\frac{\tau}{(K\,u)^2}\epsilon^2};\frac{K\,u}{\epsilon}-1\right) = \mu^{(q)}-\xi^{(q)}\epsilon+O(\epsilon^2)\end{aligned} \tag{34}$$

where $\mu^{(q)}\equiv\mu^{(q)}(\tau;K\,u)$ is obtained by expanding (14) at second order in ϵ, while $\nu^{(q)}\equiv\nu^{(q)}(\tau;K\,u)$ and $\xi^{(q)}\equiv\xi^{(q)}(\tau;K\,u)$ follow from an expansion to third order. We find explicitly

$$\mu^{(q)} = e^{\sqrt{6}w}\times\frac{9w^2\cosh^2\left(\sqrt{\frac{3}{2}}w\right)+\left(9w^2-6w\sqrt{9w^2\coth^2\left(\sqrt{\frac{3}{2}}\right)+2\tau}+2\tau\right)\sinh^2\left(\sqrt{\frac{3}{2}}w\right)}{9w^2+2\tau\sinh^2\left(\sqrt{\frac{3}{2}}w\right)}$$

with $w=K\,u$

and

$$\nu^{(q)} - \xi^{(q)} = \sqrt{6}\left(\frac{\left(e^{\sqrt{6}Ku}+1\right)\left(e^{\sqrt{6}Ku}-\mu^{(q)}\right)^3}{\left(e^{\sqrt{6}Ku}-1\right)^3\left(e^{\sqrt{6}Ku}+\mu^{(q)}\right)} - \mu^{(q)}\right) .$$

Plugging the expansion (34) in (15), we then have the scaling behavior

$$Z^{(q)}\left(e^{-\frac{\tau}{(K\,u)^2}\epsilon^2}; \frac{K\,u}{\epsilon}, \frac{K}{\epsilon}\right) \sim \zeta^{(q)}(\tau; K, u)\,\epsilon^3 ,$$

$$\zeta^{(q)}(\tau; K, u) = \left(\frac{24e^{\sqrt{6}K}\left(e^{\sqrt{6}K}+\mu^{(q)}\right)\left(\nu^{(q)} - \xi^{(q)} + \sqrt{6}\,\mu^{(q)}\right)}{\left(e^{\sqrt{6}K}-\mu^{(q)}\right)^3}\right)$$

$$= \frac{24\sqrt{6}\,e^{\sqrt{6}K}\left(e^{\sqrt{6}Ku}+1\right)\left(e^{\sqrt{6}Ku}-\mu^{(q)}\right)^3\left(e^{\sqrt{6}K}+\mu^{(q)}\right)}{\left(e^{\sqrt{6}Ku}-1\right)^3\left(e^{\sqrt{6}K}-\mu^{(q)}\right)^3\left(e^{\sqrt{6}Ku}+\mu^{(q)}\right)} . \tag{35}$$

To be consistent with the expansion (26), we need that

$$A_i^{(q)}(e^{-\frac{\tau}{(k\,u)}}; k\,u, k) \underset{k\to\infty}{\sim} k^{2i-3} \times [K^{2i-3}]\zeta^{(q)}(\tau; K, u) .$$

We deduce in particular

$$\lim_{k\to\infty} E_k(e^{-\tau L(k\,u)}) = \lim_{k\to\infty} \frac{A_3^{(q)}(e^{-\frac{\tau}{(k\,u)^2}}; k\,u, k)}{A_3^{(q)}(1; k\,u, k)} = \frac{[K^3]\zeta^{(q)}(\tau; K, u)}{[K^3]\zeta^{(q)}(0; K, u)} .$$

Using the above explicit expressions for $\mu^{(q)}$ and $\zeta^{(q)}(\tau; K, u)$ and performing a small K expansion to extract the appropriate term of order K^3, we eventually arrive at (4) with $c = 1/3$.

We can repeat the analysis for triangulations. If we use notations which parallel those introduced for quadrangulations, we find the simple correspondence

$$\mu^{(t)}(\tau; K\,u) = \mu^{(q)}\left(\frac{3\tau}{2}; \frac{2}{3^{1/4}}\,K\,u\right)$$

$$\nu^{(t)} - \xi^{(t)} = \sqrt{8\sqrt{3}}\left(\frac{\left(e^{\sqrt{8\sqrt{3}}Ku}+1\right)\left(e^{\sqrt{8\sqrt{3}}Ku}-\mu^{(t)}\right)^3}{\left(e^{\sqrt{8\sqrt{3}}Ku}-1\right)^3\left(e^{\sqrt{8\sqrt{3}}Ku}+\mu^{(t)}\right)} - \mu^{(t)}\right) .$$

$$\zeta^{(t)}(\tau; K, u) = \frac{24\sqrt{8\sqrt{3}}\,e^{\sqrt{8\sqrt{3}}K}\left(e^{\sqrt{8\sqrt{3}}Ku}+1\right)\left(e^{\sqrt{8\sqrt{3}}Ku}-\mu^{(t)}\right)^3\left(e^{\sqrt{8\sqrt{3}}K}+\mu^{(t)}\right)}{\left(e^{\sqrt{8\sqrt{3}}Ku}-1\right)^3\left(e^{\sqrt{8\sqrt{3}}K}-\mu^{t)}\right)^3\left(e^{\sqrt{8\sqrt{3}}Ku}+\mu^{(t)}\right)}$$

and

$$\lim_{k\to\infty} E_k(e^{-\tau L(k\,u)}) = \frac{[K^3]\zeta^{(t)}(\tau; K, u)}{[K^3]\zeta^{(t)}(0; K, u)} .$$

With these expressions, we arrive at the same expression (4) as for quadrangulations, but now with $c = 1/2$[17] .

This proves our second main result for quadrangulations and triangulations. To obtain the expression (5) for $\mathcal{P}(L; u)$, we simply have to compute the inverse Laplace transform of $F(\sigma(\tau; u); u)$ as given by (4). The details of this computation are presented in Appendix A.

[17]Note that the passage from quadrangulations to triangulations amounts to two simultaneous changes: $K \to 2K/3^{1/4}$ and $\tau \to 3\tau/2$. The first change has no impact on the formula for $\lim_{k\to\infty} E_k(e^{-\tau L(k\,u)})$ but the second change is responsible for the passage from $c = 1/3$ to $c = 1/2$.

5. Conclusion

In this paper, we showed how to control the hull perimeters in pointed-rooted quadrangulations or triangulations in a very explicit way by some appropriate decoration of recursion relations inherited from a decomposition of the maps via cuts appearing precisely along hull boundaries. Even though we concentrated here only on the statistics of hull perimeters, namely the lengths of hull boundaries, we could in principle measure other quantities characterizing the hulls such as for instance their volume, as was done in [2, 3].

It was recognized in [7, 6] that the structure of the hull in a random map can be understood as some particular time-reversed branching process. In our formalism, this process appears in the branching nature of the successive cuttings of the original slice encoding the pointed-rooted map at hand into smaller and smaller sub-slices. In particular, the branching information is entirely captured by the kernel of the recursion relation. In this respect, it is likely that the universal laws that we found can be given some more direct interpretation as statistical laws for appropriate quantities in the branching process.

To conclude, we would like to stress that we were eventually interested in this paper in the limit $N \to \infty$ with distances which do not scale with N. This is the so-called local limit of large maps, whose continuous description is provided by the Brownian plane [1]. If we want instead a full access to properties of the so-called scaling limit, described by the celebrated Brownian map [9, 8], we simply have to let k and d scale like $N^{1/4}$ when N becomes large. Our expressions are also well adapted to this scaling limit and it could be interesting to extend our calculations to this case.

Note finally that the notion of hull was recently shown in [10] to be a fundamental ingredient in the characterization of the Brownian map, which makes its statistical study even more appealing.

Appendix A. Inverse Laplace transforms

The quantity $\mathcal{P}(L;u)$ is simply the inverse Laplace transform of $F\left(\sigma(\tau;u);u\right)$ as given by (4), where L is the conjugate variable of τ. Assuming that we know the inverse Laplace transform $\check{F}(\ell;u)$ of $F(\sigma;u)$, where ℓ in the conjugate variable of σ, we clearly have, since $\sigma(\tau;u) = (b(u)-1) + c\,b(u) \times \tau$ (with $b(u) = (1-u)^2/u^2$):

$$\mathcal{P}(L;u) = \frac{1}{c\,b(u)}\,\check{F}\left(\frac{L}{c\,b(u)};u\right)\,e^{-\frac{b(u)-1}{c\,b(u)}\,L}\ .$$

To compute $\check{F}(\ell;u)$, we simply need the inverse Laplace transforms of the functions σ^n for $n=-4$, -3 and -2, and those of $\sigma^n/(1+\sigma)^{5/2}$ for $n=-4,-3,\cdots,+1$. The first three are respectively $\ell^3/3!$, $\ell^2/2!$ and ℓ. As for the last six, they are equal to:

$$\begin{aligned}
n=-4: &\qquad \frac{e^{-\ell}\sqrt{\ell}\,\left(4\ell^2+315\right)}{24\sqrt{\pi}} + \frac{1}{48}\left(8\ell^3-60\ell^2+210\ell-315\right)\,\mathrm{erf}\left(\sqrt{\ell}\right)\ ,\\
n=-3: &\qquad -\frac{5e^{-\ell}\sqrt{\ell}(2\ell+21)}{12\sqrt{\pi}} + \frac{1}{8}(4\ell^2-20\ell+35)\,\mathrm{erf}\left(\sqrt{\ell}\right)\ ,\\
n=-2: &\qquad \frac{e^{-\ell}\sqrt{\ell}(4\ell+15)}{3\sqrt{\pi}} + \frac{1}{2}\,(2\ell-5)\,\mathrm{erf}\left(\sqrt{\ell}\right)\ ,\\
n=-1: &\qquad -\frac{2e^{-\ell}\sqrt{\ell}(2\ell+3)}{3\sqrt{\pi}} + \mathrm{erf}\left(\sqrt{\ell}\right)\ ,\\
n=0: &\qquad \frac{4e^{-\ell}\ell^{3/2}}{3\sqrt{\pi}}\ ,\\
n=1: &\qquad -\frac{2e^{-\ell}\sqrt{\ell}(2\ell-3)}{3\sqrt{\pi}}\ .
\end{aligned}$$

Using these values, we easily evaluate

$$\check{F}(\ell;u) = \frac{u^3\sqrt{\ell}\,e^{-\ell}}{2\sqrt{\pi}}\left(\left(e^{\ell}\sqrt{\pi\,\ell}\left(1-\mathrm{erf}\left(\sqrt{\ell}\right)\right)-1\right)p(\ell)+r(\ell)\right)$$

with $p(\ell)$ and $r(\ell)$ as in (5) where $b=b(u)=(1-u)^2/u^2$. Equation (5) follows immediately.

Let us know discuss how we may obtain the expression (7) for the joint probability density $\mathcal{P}(L_1,L_2;v)$. Clearly, it is simply the result of a double inverse Laplace transform of the expression (6) where L_1 and L_2 are the conjugate variables of τ_1 and τ_2 respectively. The inverse Laplace transform in the variable L_2 is easily performed, leading to

$$2\sqrt{\frac{L_2}{\pi}}\,\frac{v^3}{c^{3/2}}\,\frac{e^{-\frac{L_2\,v^2\omega_1^2}{c((v-1)\omega_1+1)^2}}}{\left((v-1)\omega_1+1\right)^3} = \sqrt{\frac{2}{\pi}}\,\frac{(v-1)v^2}{c}\times\frac{e^{-\frac{t_2^2\,(v-1)^2\omega_1^2}{2((v-1)\omega_1+1)^2}}\,t_2}{\left((v-1)\omega_1+1\right)^3}$$
$$\text{with}\quad \omega_1\equiv\sqrt{1+c\,\tau_1}\quad\text{and}\quad t_2\equiv\sqrt{\frac{2L_2\,v^2}{c\,(v-1)^2}}\ .$$

Writing the second factor as

$$\frac{e^{-\frac{t_2^2\,(v-1)^2\omega_1^2}{2((v-1)\omega_1+1)^2}}\,t_2}{\left((v-1)\omega_1+1\right)^3} = \frac{e^{-\frac{t_2^2}{2(\Omega_1+1)^2}}t_2\Omega_1^3}{\left(\Omega_1+1\right)^3}\ ,\qquad \Omega_1\equiv\frac{1}{(v-1)\omega_1}\ ,$$

we may expand the last expression as

$$\frac{e^{-\frac{t_2^2}{2(\Omega_1+1)^2}}t_2\Omega_1^3}{\left(\Omega_1+1\right)^3} = e^{-\frac{t_2^2}{2}}\times\sum_{n=0}^{\infty}\frac{\Omega_1^{n+3}}{n!}(-1)^n\,\pi_n(t_2)$$

with $\pi_n(t)$ as in (8). This latter equation is obtained from the relation[18]

$$e^{-\frac{t_2^2}{2(\Omega_1+1)^2}} = \sum_{n=0}^{\infty}\frac{(-\Omega_1)^n}{n!}t\,\frac{\partial}{\partial t^n}\left(t^{n-1}e^{-\frac{t_2^2}{2}}\right)$$

upon differentiating with expect to Ω_1 and multiplying by (Ω_1^3/t_2). We may now use the inverse Laplace transform:

$$\Omega_1^{n+3} = \frac{1}{(v-1)^{n+3}}\,\frac{1}{\left(1+c\,\tau_1\right)^{\frac{n+3}{2}}}\quad\xrightarrow{\text{Inv. Laplace Trans.}}\quad\frac{e^{-\frac{L_1}{c}}\left(\frac{L_1}{c(v-1)^2}\right)^{\frac{n+3}{2}-1}}{c\,(v-1)^2\,\Gamma\left(\frac{n+3}{2}\right)}\ .$$

Incorporating this formula in our infinite sum, we end up with

$$\mathcal{P}(L_1,L_2;v) = \sqrt{\frac{2}{\pi}}\,\frac{(v-1)v^2}{c}\times e^{-\frac{t_2^2}{2}}\times\sum_{n=0}^{\infty}\frac{1}{n!}\,\frac{e^{-\frac{L_1}{c}}\left(\frac{L_1}{c(v-1)^2}\right)^{\frac{n+3}{2}-1}}{c\,(v-1)^2\,\Gamma\left(\frac{n+3}{2}\right)}(-1)^n\,\pi_n(t_2)\ ,$$

which is precisely (7).

[18]Using the Leibniz formula to compute the n-th derivative and rearranging the terms, the right hand side in the relation is indeed easily rewritten as the shift operator $\sum_{n=0}^{\infty}\frac{a^n}{n!}\frac{\partial^n}{\partial t^n}f(t)=f(t+a)$ acting on the function $f(t)=e^{-t^2/2}$ with $a=-t\,\Omega_1/(\Omega_1+1)$.

Appendix B. First terms of the g-expansion of $Z^{(q)}(\alpha;d,k)$ and $Z^{(t)}(\alpha;d,k)$

We give here the first terms of the g-expansion of $Z^{(q)}(\alpha;d,k)$ (up to order g^8) and of $Z^{(t)}(\alpha;d,k)$ (up to order g^{12}) for the smallest values of d and k allowed in our formulas. The coefficients of $\alpha^{\mathcal{L}}\, g^N$ in these expansions are the *numbers* of k-pointed-rooted quadrangulations (respectively triangulations) with a given number N of faces and a fixed value $\mathcal{L}$ of the hull perimeter $\mathcal{L}(d)$. We find:

$$\begin{aligned}
Z^{(q)}(\alpha;2,3) &= \alpha^2 g^2+15\alpha^2 g^3+\alpha^2\left(\alpha^2+178\right) g^4+7\alpha^2\left(4\alpha^2+281\right) g^5\\
&\quad+\alpha^2\left(\alpha^4+518\alpha^2+21165\right) g^6+\left(42\alpha^6+8018\alpha^4+225488\alpha^2\right) g^7\\
&\quad+\alpha^2\left(\alpha^6+1075\alpha^4+112671\alpha^2+2395983\right) g^8+O\left(g^9\right)\\
Z^{(q)}(\alpha;2,4) &= \alpha^2 g^3+22\alpha^2 g^4+\left(\alpha^4+342\alpha^2\right) g^5+\left(36\alpha^4+4640\alpha^2\right) g^6\\
&\quad+\left(\alpha^6+815\alpha^4+58799\alpha^2\right) g^7+\left(51\alpha^6+14914\alpha^4+716865\alpha^2\right) g^8+O\left(g^9\right)\\
Z^{(q)}(\alpha;3,4) &= \alpha^2 g^3+22\alpha^2 g^4+\alpha^2\left(2\alpha^2+341\right) g^5+\alpha^2\left(71\alpha^2+4605\right) g^6\\
&\quad+\alpha^2\left(3\alpha^4+1586\alpha^2+58026\right) g^7+5\alpha^2\left(30\alpha^4+5731\alpha^2+140605\right) g^8+O\left(g^9\right)\\
Z^{(q)}(\alpha;2,5) &= \alpha^2 g^4+29\alpha^2 g^5+\left(\alpha^4+555\alpha^2\right) g^6+\left(43\alpha^4+8876\alpha^2\right) g^7\\
&\quad+\left(\alpha^6+1127\alpha^4+128712\alpha^2\right) g^8+O\left(g^9\right)\\
Z^{(q)}(\alpha;3,5) &= \alpha^2 g^4+29\alpha^2 g^5+2\alpha^2\left(\alpha^2+277\right) g^6+\left(87\alpha^4+8832\alpha^2\right) g^7\\
&\quad+\alpha^2\left(3\alpha^4+2300\alpha^2+127537\right) g^8+O\left(g^9\right)\\
Z^{(q)}(\alpha;4,5) &= \alpha^2 g^4+29\alpha^2 g^5+2\alpha^2\left(\alpha^2+277\right) g^6+\alpha^2\left(86\alpha^2+8833\right) g^7\\
&\quad+\alpha^2\left(3\alpha^4+2251\alpha^2+127586\right) g^8+O\left(g^9\right)
\end{aligned}$$

and

$$\begin{aligned}
Z^{(t)}(\alpha;1,2) &= \alpha g^2+\alpha(\alpha+14) g^4+\alpha\left(\alpha^2+26\alpha+199\right) g^6+\alpha\left(\alpha^3+39\alpha^2+533\alpha+2952\right) g^8\\
&\quad+\alpha\left(\alpha^4+53\alpha^3+1062\alpha^2+10147\alpha+45473\right) g^{10}\\
&\quad+\alpha\left(\alpha^5+68\alpha^4+1824\alpha^3+25040\alpha^2+187756\alpha+722498\right) g^{12}+O\left(g^{14}\right)\\
Z^{(t)}(\alpha;1,3) &= \alpha g^4+\alpha(\alpha+28) g^6+\alpha\left(\alpha^2+42\alpha+612\right) g^8+\alpha\left(\alpha^3+57\alpha^2+1220\alpha+12326\right) g^{10}\\
&\quad+\alpha\left(\alpha^4+73\alpha^3+2090\alpha^2+30456\alpha+239793\right) g^{12}+\alpha+O\left(g^{14}\right)\\
Z^{(t)}(\alpha;2,3) &= \alpha g^4+\alpha(2\alpha+27) g^6+\alpha\left(3\alpha^2+79\alpha+573\right) g^8+\alpha\left(4\alpha^3+159\alpha^2+2178\alpha+11263\right) g^{10}\\
&\quad+\alpha\left(5\alpha^4+270\alpha^3+5479\alpha^2+51970\alpha+214689\right) g^{12}+O\left(g^{14}\right)\\
Z^{(t)}(\alpha;1,4) &= \alpha g^6+\alpha(\alpha+42) g^8+\alpha\left(\alpha^2+56\alpha+1225\right) g^{10}\\
&\quad+\alpha\left(\alpha^3+71\alpha^2+2031\alpha+30792\right) g^{12}+O\left(g^{14}\right)\\
Z^{(t)}(\alpha;2,4) &= \alpha g^6+\alpha(2\alpha+41) g^8+\alpha\left(3\alpha^2+111\alpha+1168\right) g^{10}\\
&\quad+\alpha\left(4\alpha^3+213\alpha^2+3984\alpha+28694\right) g^{12}+O\left(g^{14}\right)\\
Z^{(t)}(\alpha;3,4) &= \alpha g^6+\alpha(2\alpha+41) g^8+\alpha\left(3\alpha^2+108\alpha+1171\right) g^{10}\\
&\quad+\alpha\left(4\alpha^3+204\alpha^2+3791\alpha+28896\right) g^{12}+O\left(g^{14}\right)\ .
\end{aligned}$$

Appendix C. General expression for the average hull perimeter

We give here for information the expression of $E_k(\mathcal{L}(d))$ at *finite* k *and* d, for both quadrangulations (satisfying $E_k(\mathcal{L}(d))=\frac{\partial}{\partial\alpha}W_k^{(q)}(\alpha;d)|_{\alpha=1}$) and triangulations ($E_k(\mathcal{L}(d))=$

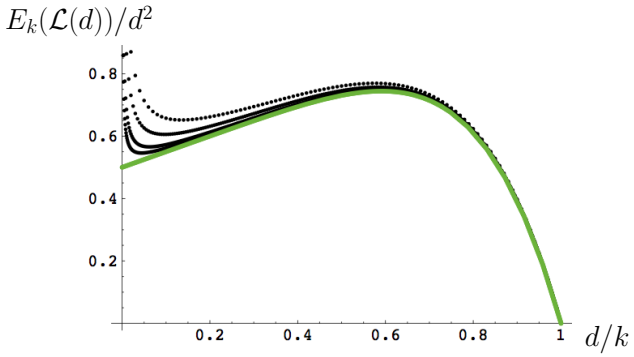

FIGURE 16. A plot of $E_k(\mathcal{L}(d))/d^2$ for quadrangulations as a function of d/k for $k = 100$, 200, 500 and 1000 (from top to bottom), and the scaling limit $L_{\mathrm{av}}(d/k)$ (green line).

$\frac{\partial}{\partial\alpha}W_k^{(t)}(\alpha;d)|_{\alpha=1}$). In the case of quadrangulations, we find:

$$E_k(\mathcal{L}(d)) = \frac{k(k+1)(k+2)}{2\,(k^2+2k-1)\,(5k^4+20k^3+27k^2+14k+4)}\times$$
$$\times\left((d-1)(d+1)(d+2)(d+4)(2k+3)\times\right.$$
$$\times\frac{\left((1-d)(d+1)(d+2)(d+4)\left(5d^2+15d+17\right)+(k+1)^2(k+2)^2\left(5k^2+15k+2\right)-4\right)}{3(2d+3)(k+1)^2(k+2)^2}$$
$$-(d-2)d(d+1)(d+3)(2k+1)\times$$
$$\left.\times\frac{\left((2-d)d(d+1)(d+3)\left(5d^2+5d+7\right)+k^2(k+1)^2\left(5k^2+5k-8\right)-4\right)}{3(2d+1)k^2(k+1)^2}\right).$$

for $2 \le d < k$. This quantity, rescaled by d^2, is plotted in figure 16 to emphasize its scaling limit at large k and d.

In the case of triangulations, we find instead:

$$E_k(\mathcal{L}(d)) = \frac{k^2(k+1)^2}{2(2k+1)\,(5k^6+15k^5+14k^4+3k^3-k^2-1)}\times$$
$$\times\left(\frac{d(d+1)(d+2)(d+3)\left(10(k+1)^6-7(k+1)^4-2d(d+1)(d+2)(d+3)\left(5d^2+15d+14\right)-2\right)}{(k+1)^3(2d+3)}\right.$$
$$\left.-\frac{(d-1)d(d+1)(d+2)\left(10k^6-7k^4-2(d-1)d(d+1)(d+2)\left(5d^2+5d+4\right)-2\right)}{k^3(2d+1)}\right).$$

for $1 \le d < k$.

ACKNOWLEDGEMENTS

The author acknowledges the support of the grant ANR-14-CE25-0014 (ANR GRAAL).

REFERENCES

[1] N. Curien and J-F. Le Gall. The brownian plane. *Journal of Theoretical Probability*, 27(4):1249–1291, 2013.
[2] N. Curien and J-F Le Gall. The hull process of the brownian plane, 2014. arXiv:1409.4026 [math.PR].
[3] N. Curien and J-F Le Gall. Scaling limits for the peeling process on random maps, 2014. arXiv:1412.5509 [math.PR].

[4] E. Guitter. The distance-dependent two-point function of quadrangulations: a new derivation by direct recursion, 2015. arXiv:1512.00179 [math.CO].
[5] E. Guitter. The distance-dependent two-point function of triangulations: a new derivation from old results, 2015. arXiv:1511.01773 [math.CO].
[6] M.A. Krikun. Local structure of random quadrangulations, 2005. arXiv:math/0512304 [math.PR].
[7] M.A. Krikun. Uniform infinite planar triangulation and related time-reversed critical branching process. *Journal of Mathematical Sciences*, 131(2):5520–5537, 2005.
[8] J-F. Le Gall. Uniqueness and universality of the brownian map. *Ann. Probab.*, 41(4):2880–2960, 2013.
[9] G. Miermont. The brownian map is the scaling limit of uniform random plane quadrangulations. *Acta Mathematica*, 210(2):319–401, 2013.
[10] J. Miller and S. Sheffield. An axiomatic characterization of the brownian map, 2015. arXiv:1506.03806 [math.PR].

Institut de Physique Théorique, CEA, IPhT, 91191 Gif-sur-Yvette, France, CNRS, UMR 3681
E-mail address: emmanuel.guitter@cea.fr